

# Advancements and Perspectives in Folate-Based Anticancer Drugs: Bridging Quantum and Classical Mechanics in Folate Receptor Research

Andrea Jess Josiah, Krishna Kuben Govender,\* Penny Poomani Govender,  
and Suprakas Sinha Ray\*

This review highlights the role of computational chemistry, specifically quantum and molecular mechanics, in the development of folate-based anticancer drugs. Folate receptors (FRs) are overexpressed in cancerous cells, rendering these receptors a key focus in the design of targeted drug delivery systems. These computational tools are fundamental for analyzing drug–receptor interactions and overcoming the limitations of traditional drug development processes. A 10-year literature survey demonstrated advancements in employing FRs for targeted cancer therapy. Key findings reveal that structural modifications to folate derivatives consistently enhance binding affinities and specificity toward FR $\alpha$  and FR $\beta$ . Computational methodologies predicted and analyzed molecular interactions, validated by experimental data. Functional groups play a crucial role in enhancing binding stability and interaction strength within FR binding pockets. Detailed structural insights into folate derivatives and antifolates interacting with FRs have identified critical residues involved in binding, aiding the design of targeted therapeutics.

which is an essential element required in various biological processes. These processes include the synthesis of RNA and DNA, cellular division and subsequent proliferation, and hematopoiesis.<sup>[1]</sup> The terms “folic acid” and “folate” are frequently used interchangeably; however, FA is not naturally occurring.<sup>[2]</sup>

Folate receptors (FRs) enable the connection between fundamental biochemical functions of FA and several cellular processes through FR isoforms and unique structural characteristics.<sup>[3]</sup> Folate receptors are classified as glycoproteins and comprise  $\approx$ 240–260 amino acids<sup>[4]</sup> with a relative molecular weight of 35–40 kDa.<sup>[5]</sup> These FRs are categorized into four isoforms, namely FR $\alpha$ , FR $\beta$ , FR $\gamma$ , and FR $\delta$ .<sup>[6]</sup> Isoforms ( $\alpha$ ,  $\beta$ , and  $\delta$ ) are transmembrane proteins attached to the cell surface via glycosylphosphatidylinositol (GPI) anchors.

Conversely, the FR $\gamma$  isoform lacks the GPI anchor, resulting in detachment from the cell surface.<sup>[1]</sup> These isoforms are biologically multifunctional, playing a role in the synthesis, methylation, repair, and cell division of DNA. Additionally, FRs are involved in subcellular localizations and tissue-specific expression patterns.<sup>[7]</sup>

Folate receptors have attracted significant interest in targeted drug delivery strategies for epithelial carcinomas, primarily attributed to the disparity in FR expression levels between cancerous and non-cancerous cells.<sup>[8]</sup> Literature indicates the up-regulation of FRs in various carcinomas, which include the lung, kidney, brain, ovary, colon, breast, and myeloid cells.<sup>[9]</sup> However, FRs exhibit low levels of expression in non-malignant cells, comparatively<sup>[8]</sup>; consequently, FRs can be considered a potential tumor biomarker.<sup>[10]</sup>

In pharmaceutical R&D, traditional trial-and-error experiments frequently result in unsatisfactory outcomes, necessitating re-evaluation and re-testing. These conventional methods contribute to the unpredictability and time and capital-intensive development process.<sup>[11]</sup> In a recent review, the UK Research and Innovation-Biotechnology and Biological Sciences Research Council (UKRI-BBSRC) highlighted the challenges of managing large-scale, complex data within pharmaceutical development.<sup>[12]</sup> Furthermore, the research council presented a viable strategy that involves leveraging advancements in computing and

## 1. Introduction

Folic acid (FA), chemically represented as (C<sub>19</sub>H<sub>19</sub>N<sub>7</sub>O<sub>6</sub>), is alternatively known as (pteroyl-L-glutamic acid) a B9 vitamin,

A. J. Josiah, S. Sinha Ray  
Centre for Nanostructured and Advanced Materials  
DSI-CSIR Nanotechnology Innovation Centre  
Council for Scientific and Industrial Research  
Pretoria 0001, South Africa  
E-mail: rsuprakas@csir.co.za, ssinharay@uj.ac.za

A. J. Josiah, K. K. Govender, P. P. Govender, S. Sinha Ray  
Department of Chemical Sciences  
University of Johannesburg  
Johannesburg 2028, South Africa  
E-mail: krishnag@uj.ac.za

The ORCID identification number(s) for the author(s) of this article can be found under <https://doi.org/10.1002/adts.202400377>

© 2024 The Author(s). Advanced Theory and Simulations published by Wiley-VCH GmbH. This is an open access article under the terms of the [Creative Commons Attribution](#) License, which permits use, distribution and reproduction in any medium, provided the original work is properly cited.

DOI: 10.1002/adts.202400377

algorithms for computational analysis and modeling. Adopting a data-intensive approach focused on enhancing the findability, accessibility, interoperability, and reusability of data can potentially benefit pharmaceutical R&D. This strategy promises to streamline the handling of extensive, varied datasets, driving innovations in drug development.<sup>[12]</sup> A review by Lin et al.,<sup>[13]</sup> indicated that the rapid evolution of computer hardware, software, and algorithms has significantly propelled advancements in drug design and development. These improvements have facilitated the integration of various computational methods that are time and cost-efficient in the drug development process.

Theoretical chemistry describes the fusion between mathematical methods with principles of quantum or classical mechanics, forming a strategic approach for analyzing and understanding chemical systems. Computational chemistry emerges as a sub-discipline, characterized by applying theoretical chemical concepts via advanced software tools.<sup>[14]</sup> Two integral components in computational chemistry are quantum mechanics (QM) and molecular mechanics (MM) calculations, which are employed to analyze and predict the molecular structure and behavior of chemical compounds.

These computational techniques have revolutionized the drug development process, enabling researchers to study and understand the interactions between a drug and its corresponding molecular target. In the case of FRs, QM and MM have been extensively used to gain insights into the interactions between folate-based drugs and their respective receptors. These studies have provided valuable information on the binding affinity, conformational changes, and energetics of drug–receptor interactions, aiding the design and optimization of novel folate-based drug systems.

This review critically examines the use of QM and MM in FRs and folate-based drugs. It assesses the contribution of QM calculations to understanding drug–receptor interactions, evaluates the accuracy of these methods, and compares them with MM approaches. Additionally, this review discusses the advantages and limitations of QM and MM, identifying current trends and potential future directions in computational pharmacology. This approach aims to provide a comprehensive and critical analysis of the efficacy and applicability of QM and MM methods in this research area.

## 2. Drug Discovery and Development

Drug discovery is characterized as a financially intensive and technically complex process.<sup>[15]</sup> Daina et al.,<sup>[16]</sup> reported that the timeline for new drug development from inception to market launch is  $\approx 10$ – $15$  years, with associated costs of  $\approx 2.6$  billion US dollars (Figure 1).<sup>[17]</sup> The discovery and development of new drugs involve a comprehensive five-stage process. The pre-discovery or target identification phase includes extensive biological and genetic data analysis to understand disease mechanisms and identify potential targets.<sup>[18]</sup> Subsequently, the drug discovery stage entails screening various molecules to determine those that demonstrate a therapeutic benefit. The preclinical development stage focuses on elucidating the mode of action of drug candidates, assessing potential toxicity, and validating efficacy through *in vitro* and *in vivo* models. The formulation evaluation stage employs a plethora of technologies and

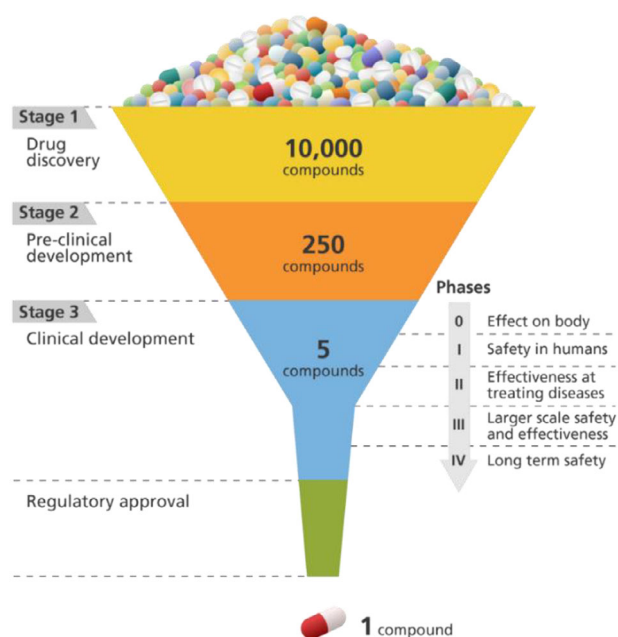


**Figure 1.** Stages of drug development.<sup>[17]</sup> This is an open-access image distributed under the terms of the Creative Commons CC BY license.

methodologies, including high-throughput screening, medicinal chemistry, and various omics technologies, to systematically refine hits into potent and selective drug candidates through lead optimization. The clinical stage involves rigorous testing of these candidates to assess safety and efficacy in a practical setting. The final stage includes regulatory review, approval, and post-market surveillance to ensure the long-term safety and effectiveness of the drug upon market entry.<sup>[15]</sup> The integration of computational chemistry into drug discovery streamlines the identification and optimization of candidates through virtual screening and rational molecule design. This method efficiently predicts compound efficacy and safety, reducing traditional development cycles. By elucidating molecular disease mechanisms and drug interactions, it accelerates drug discovery, enhancing time and cost efficiency.<sup>[19]</sup>

## 3. Overview of Drug Receptor Theories

The development of receptor theories is fundamental to understanding the molecular mechanisms responsible for drug action.<sup>[20]</sup> The foundational concept, by Langley and Ehrlich, explains that drug compounds exert a biological effect upon binding to specific sites on cells. This concept describes the “lock and key” model, where the drug (key) binds to a specific receptor (lock) to elicit a biological response.<sup>[21]</sup> Receptors are defined as a protein or a protein complex located intracellularly, extracellularly, or in both cellular environments.<sup>[22]</sup> A biological response is triggered upon the interaction of a drug and molecular target, which can result in either a therapeutic or adverse effect.<sup>[23]</sup> Furthermore, current theories recognize that receptor binding can exhibit various outcomes, beyond the activation or inhibition of a biological process.<sup>[24]</sup> The concepts of agonism, antagonism, partial agonism, and inverse agonism,

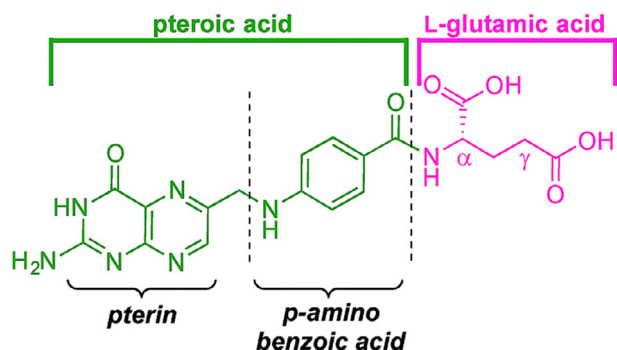


**Figure 2.** Molecular structure of folic acid.<sup>[29]</sup> This is an open-access article distributed under the terms of the Creative Commons CC BY license.

describe diverse effects, reflecting the dynamic nature of receptor–drug interactions.<sup>[25]</sup> A pivotal factor influencing receptor binding outcomes is receptor selectivity, which evaluates the binding of a ligand to multiple receptors and subsequently identifies the optimal receptor depending on binding affinity.<sup>[26]</sup> Consequently, binding affinity plays a significant role in the pharmacodynamics and pharmacokinetics of a drug. A higher binding affinity between a receptor and the corresponding ligand results in a lower required drug concentration to achieve full saturation.<sup>[27]</sup>

Studies focusing on receptor and ligand analysis have been revolutionized by the integration of MM and QM methods, due to the visualization and manipulation of receptors at the atomic level. This advancement has facilitated more accurate predictions of drug–receptor interactions, contributing to the development of more efficacious and safer pharmaceuticals.

### 3.1. Molecular Structure of Folic Acid and Mechanisms of Cellular Internalization

Folic acid has a molecular structure that can be segmented into three constituents. The initial constituent is a heterocyclic pteridine moiety composed of two rings connected to the second constituent, para-aminobenzoic acid (PABA), via a methylene bridge at carbon 6. The third constituent is a glutamic acid moiety joined via an amide bond<sup>[28]</sup> (Figure 2)

The glutamic acid residue contains two carboxylic groups that are deprotonated at a physiological pH of 7.4.<sup>[30]</sup> Folates are internalized into cells through receptor-mediated endocytosis facilitated by FR $\alpha$ . This process initiates the formation of an endocytic vesicle, following the plasma membrane's encapsulation of the receptor–ligand complex. The receptor–ligand complex subsequently navigates through intracellular organelles such as early endosomes and compartments for uncoupling of receptor and ligand (CURLs).<sup>[31]</sup> The dissociation of the receptor–ligand complex is facilitated by CURL and is expedited by the reduction in pH to  $\approx 5$ . Thereafter, the late endosome and lysosome fuse, resulting in the cytotoxic drug being released into the cell. The receptors are routed to the recycling endosome for either degradation or re-expression on the cell surface, enabling subsequent rounds of endocytosis.<sup>[32]</sup>

### 3.2. Molecular Interplay between Folate Receptors and Folic Acid

The pteric acid moiety of FA binds to the FR, which is a deep, negatively charged pocket. The glutamic acid residue extends out of the pocket, providing a site for drug attachment.<sup>[33]</sup> An inherent characteristic of FRs is the high binding affinity toward FA and its metabolically active derivatives which include, dihydrofolate, tetrahydrofolic acid, and 5-methyltetrahydrofolate.<sup>[3]</sup> In epithelial carcinomas FR $\alpha$  is predominantly expressed compared to the other isoforms, leading to an increased binding affinity for FA.<sup>[9]</sup> The up-regulation of FR $\alpha$  expression is attributed to a phenomenon associated with tumorigenesis. During this process, the cell structure is adversely affected, leading to disorganized vasculature, breakdown of intercellular junctions, and reduced adhesion among endothelial cells. As a result, the polarized cellular localization of FR $\alpha$  is compromised, causing an erratic distribution of FR $\alpha$  throughout the cell membrane.<sup>[31]</sup> This cascade of events culminates with greater accessibility of FR $\alpha$  to drug compounds and/or drug conjugates in the circulatory system, rendering FR $\alpha$  a promising candidate for targeted cancer therapies.<sup>[34]</sup> (Figure 3)

The disruption in cell polarization of FR $\alpha$ , coupled with an elevated binding affinity toward FA, has generated substantial interest in developing drug conjugates where FA functions as a targeting ligand.<sup>[28]</sup> Employing FA as a targeting ligand provides several advantages, including low molecular weight, enhanced tissue permeability, increased stability in both acidic and alkaline environments, cost-effective, non-immunogenic, and versatility in conjugation with various organic molecules, nanoparticles (NPs), and antibodies.<sup>[35]</sup> Moreover, FA plays a fundamental role in the viability of both cancerous and non-cancerous cells, with a heightened significance in malignant cells, which depend on FA for their uncontrolled and rapid proliferation. This critical function arises from FA's involvement in intracellular one-carbon methylation reactions and nucleotide base synthesis.<sup>[10]</sup>

## 4. Theoretical Background

Structure-based drug design (SBDD) and ligand-based drug design (LBDD) are fundamental strategies in pharmaceutical research for developing novel drugs.<sup>[37]</sup> Computer-Aided Drug Design (CADD) is a key element that integrates with both SBDD and LBDD, improving the efficiency and effectiveness of drug development.<sup>[38]</sup>

SBDD relies on 3D structures of biological targets, predominantly proteins or nucleic acids, to facilitate the discovery and optimization of new drug compounds.<sup>[39]</sup> The SBDD method identifies a biological molecule associated with a disease as the target. Thereafter, a 3D structure of this drug target is obtained via X-ray crystallography, NMR spectroscopy, or cryo-electron microscopy.<sup>[40]</sup> Subsequent analysis focuses on designing molecules that accurately fit into the binding site of the target, followed by the analysis of molecular interactions between the designed molecule/s and the target site.<sup>[41]</sup> This is achieved through molecular modeling, docking simulations, and virtual screening. The final step comprises the synthesis and biological activity testing of these drug compounds.<sup>[42]</sup>

Conversely, LBDD is employed when the structural details of a target are unknown. The LBDD approach first identifies

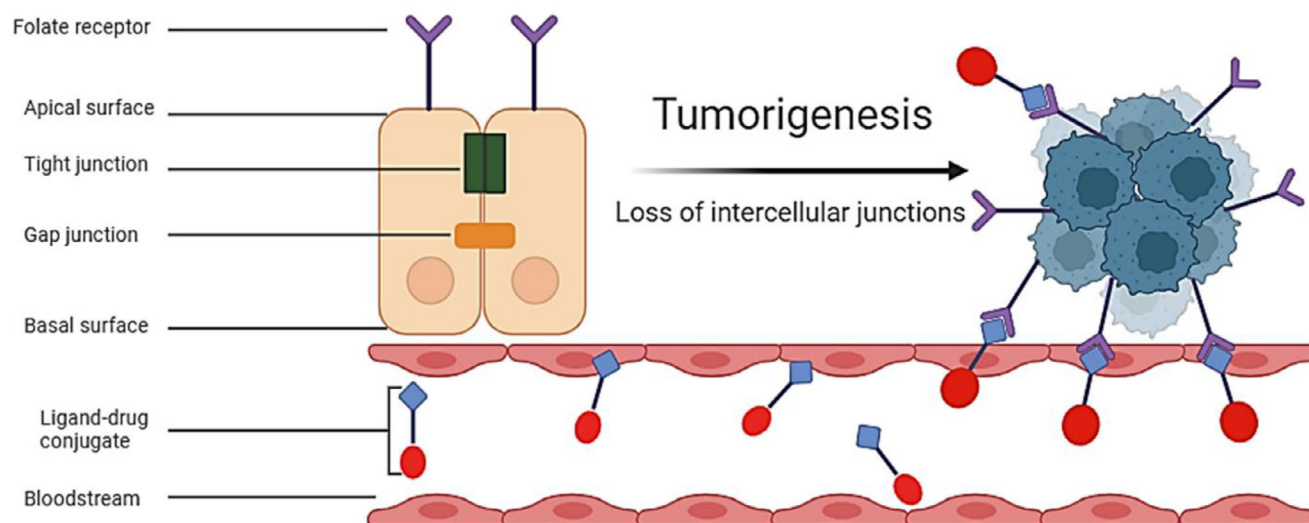


**Figure 3.** The effect of tumorigenesis on increased folate receptor availability. Adapted from,<sup>[5]</sup> created with Biorender.com.<sup>[36]</sup> This is an open-access article distributed under the terms of the Creative Commons CC BY license.

ligands exhibiting biological activity, followed by a structure–activity relationship (SAR) analysis of known ligands.<sup>[43]</sup> Molecular databases are screened to identify new compounds that demonstrate comparable biological activities. The data acquired enables the prediction of potential drug candidates without direct knowledge of the target structure. This approach employs various techniques including quantitative structure–activity relationship (QSAR) modeling, machine learning, and pharmacophore modeling.<sup>[44]</sup>

#### 4.1. Key Tools in Computational Chemistry

Computational chemistry fundamentally employs two key approaches: classical mechanics and quantum mechanics.<sup>[45]</sup> Within these approaches, there are five distinct methods. The classical mechanics approach includes MM and molecular dynamics (MD) calculations. In contrast, the QM approach encompasses Ab Initio, semi-empirical, and density functional theory (DFT) methods.<sup>[14]</sup>

#### 4.2. Classical Mechanics

Classical mechanics forms a fundamental basis point in molecular docking and molecular dynamics simulations (MDS).

Molecular mechanics is based on a mathematical model that utilizes the ball-spring model to represent molecules, where atoms are linked by bonds resembling springs.<sup>[46]</sup> A central function of MM is geometry optimization calculations, which identify a molecular configuration with the lowest energy. These calculations are achieved by several factors, including knowledge of the standard spring length, the interconnecting angles, and the energy expenditure required for bond extension or compression.<sup>[47]</sup> Molecular mechanics methods can be referred to as forcefield methods, as the parameters within the mathematical expression for energy constitute a forcefield.<sup>[48]</sup> However, the MM method

does not consider electrons; therefore, various electronic properties such as electrophilic or nucleophilic behavior and charge distribution are not accounted for. Molecular mechanics is a rapid and efficient method capable of accommodating large molecules without necessitating significant computational resources.<sup>[49]</sup>

The MM expression leverages the potential energy function and includes several principles, the Coulomb interaction between rigid point charges, a Lennard–Jones-type van der Waals term, and bonded terms<sup>[50]</sup> (bond stretching, angle bending, torsions, out-of-plane deformations, or improper torsions):

$$\begin{aligned} \text{EMM} = & \sum_{\text{bonds}} k_b (d - d_0)^2 + \sum_{\text{angles}} k_\theta (\theta - \theta_0)^2 + \sum_{\text{dihedrals}} k_\varphi [1 + \cos(n\vartheta + \delta)] \\ & + \sum_{\text{non-bonded pairs}} \left\{ \epsilon_{AB} \left[ \left( \frac{\sigma_{AB}}{\gamma_{AB}} \right)^{12} - \left( \frac{\sigma_{AB}}{\gamma_{AB}} \right)^6 \right] + \frac{1}{4\pi\epsilon_0} \frac{q_A q_B}{\gamma_{AB}} \right\} \end{aligned} \quad (1)$$

where key parameters include  $d$  for bond distance,  $\theta$  for bond angle, and  $\vartheta$  for bond torsion, describing the spatial configuration of atoms. Equilibrium states are represented by  $d_0$  and  $\theta_0$ , with  $n$  indicating torsion multiplicity and  $\delta$  the torsion phase. The force constants for bonds, angles, and torsions are  $k_b$ ,  $k_\theta$ , and  $k_\varphi$ , respectively. Non-bonded interactions are described by distance  $r_{AB}$  and Van der Waals parameters  $\epsilon_{AB}$  and  $\sigma_{AB}$ , while electrostatic interactions involve atomic partial charges  $q_A$  and  $q_B$ , and  $\epsilon_0$  denotes vacuum permittivity. These elements collectively define the forces and energies in molecular simulations.

##### 4.2.1. Molecular Docking

Molecular docking predicts the optimal binding mode of a ligand to a protein by generating potential conformations or orientations within the protein's binding site. The process involves sampling, which explores the conformational space, and scoring, which evaluates and selects the most probable binding modes.

**Table 1.** Comparative analysis of the advantages and disadvantages of various scoring functions in molecular docking.

| Scoring function | Advantages  | Disadvantages  |
|------------------|---|--|
| Force-field      | <ul style="list-style-type: none"> <li>Based on physics principles and molecular mechanics force fields.</li> <li>Considers detailed interactions, e.g. van der Waals forces and electrostatics.</li> <li>Provides a realistic representation of molecular interactions.</li> </ul> | <ul style="list-style-type: none"> <li>May oversimplify complex interactions.</li> <li>Limited accuracy in predicting binding affinities.</li> </ul>   |
| Knowledge-based  | <ul style="list-style-type: none"> <li>Derived from statistical analyses of known protein–ligand complexes.</li> <li>Uses experimental data to predict binding affinities.</li> <li>Ability to capture specific interactions observed in experimental structures.</li> </ul>        | <ul style="list-style-type: none"> <li>Limited by the availability and quality of training data.</li> <li>May not generalize well to novel ligands or targets.</li> <li>Vulnerable to biases in the training dataset.</li> </ul>                               |
| Empirical        | <ul style="list-style-type: none"> <li>Incorporate various empirical energy terms to predict binding affinities.</li> <li>Ability to be optimized to reproduce experimental binding data.</li> <li>Provides a balance between accuracy and computational efficiency.</li> </ul>     | <ul style="list-style-type: none"> <li>Reliance on empirical parameters may limit generalizability.</li> <li>May not capture all relevant interactions in complex systems.</li> <li>Optimization of coefficients can be challenging and subjective.</li> </ul> |

Three primary scoring functions are used in molecular docking: force field-based, knowledge-based, and empirical. Each type of scoring function has its strengths and limitations, and the choice of scoring function depends on the specific requirements of the docking study, the nature of the ligand–protein interaction, and the available computational resources. Researchers often employ a combination of scoring functions or tailor them to the specific system under investigation to enhance the accuracy of predictions (Table 1).

#### 4.2.2. Molecular Dynamics

Since the inception of molecular dynamics (MD) simulations in the 1970s, the field has witnessed remarkable progress.<sup>[51]</sup> Initially, simulations were limited to biological systems comprising only a few hundred atoms. Today, state-of-the-art MD simulations can encompass systems with  $\approx 50\,000$  to  $100\,000$  atoms. Moreover, with the appropriate computational resources, simulating systems containing up to  $500\,000$  atoms is feasible. This significant advancement is largely attributed to the integration of high-performance computing (HPC) technologies.<sup>[52]</sup>

Molecular Dynamics calculations implement molecular laws of motion, enabling the simulation of molecular conformational alterations or movements in response to force fields.<sup>[53]</sup> In biochemical research, MD simulations predominantly involve molecular motion driven by forces computed by MM.<sup>[54]</sup> Typically, an atomistic model is employed to represent all interacting particles at the atomic level, encompassing both solute and solvent molecules. This model is positioned within a simulation box sufficiently large to fully contain the system. The dynamics of the interactions between the solute and solvent are governed by Newton's laws of motion.<sup>[55]</sup> Specifically, the equations of motion are given by:

$$\frac{d^2 r_i(t)}{dt^2} = \frac{F_i(t)}{m_i} \quad (2)$$

where  $F_i(t)$  is the force acting on the  $i$ -th particle at time  $t$ ,  $m_i$  is the mass of the  $i$ -th particle, and  $r_i(t)$  is the position of  $i$ -th particle at time  $t$ .

Furthermore, velocity–Verlet or leap-frog are algorithms used to iteratively update the state of the model system across several time steps, resulting in a temporal evolution simulation.<sup>[56]</sup>

$$r_i(t + \delta t) = r_i(t) + v_i(t) \delta t + \frac{1}{2} a_i(t) \delta t^2 \quad (3)$$

$$v_i(t + \delta t) = v_i(t) + \frac{1}{2} [a_i(t) + a_i(t + \delta t)] \delta t \quad (4)$$

When defining a model system, a primary concern is the representation of solvent molecules.<sup>[57]</sup> Previous studies indicate that explicit representation of solvent molecules is the most effective approach, despite the resultant increase in the size and complexity of the simulated system.<sup>[58,59]</sup>

### 4.3. Quantum Mechanics

#### 4.3.1. Relationship between energy and structure

In theoretical calculations, the primary objective is to ascertain the optimal molecular structure which is characterized by its lowest energy state referred to as a minimum energy.<sup>[45]</sup> This foundational understanding enables the derivation of numerous chemical and physical properties. A central concept to this research discipline, particularly molecular dynamics, and reaction mechanisms within chemical physics, is the Potential Energy Surface (PES). A PES is a mathematical representation that describes the energy of a system, typically a set of atoms or molecules, as a function of their geometrical arrangement.<sup>[60]</sup>

A PES model is described as a multidimensional landscape, where each point represents an atomic or molecular configuration, with each elevation point indicating the potential energy that

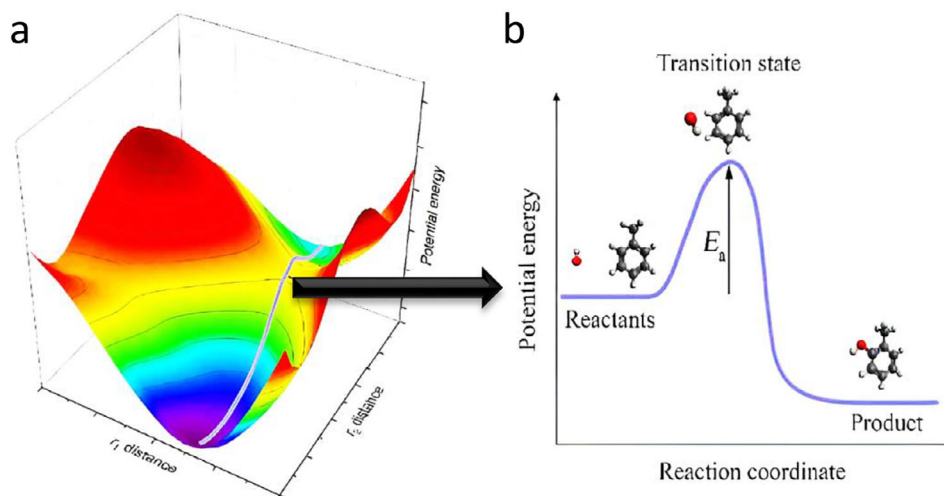


**Figure 4.** a) The Potential Energy Surface (PES) landscape and b) represents a reaction path.<sup>[63]</sup> This is an open-access article distributed under the terms of the Creative Commons CC BY license.

corresponds to a specific configuration.<sup>[61]</sup> The PES model identifies stable structures by an energy minimum and high-energy configurations by an energy maximum. Additionally, it highlights saddle points, defined as locations on the function's surface where the gradient is zero, however, these points are neither local maxima nor minima.<sup>[62]</sup> These points represent transition states (TS), which indicate the lowest energy barriers between two minima, corresponding to different isomers in a single-molecule system. A TS is key in outlining isomerization pathways. Moreover, in systems involving molecular association or dissociation, the potential for systematically mapping reaction mechanisms, including reactants, intermediates, and products, is established<sup>[45]</sup> (Figure 4a,b).<sup>[63]</sup> Therefore, PES provides a direct link between structures and energies.

#### 4.3.2. Concepts of the Quantum Mechanics Approach

The core concept in the QM approach is the wavefunction, derived from the Schrödinger equation, expressed as  $\hat{H}\Psi = E\Psi$ . Where  $\hat{H}$  represents the Hamiltonian operator, the wavefunction is denoted by  $\Psi$  and is dependent on the spatial coordinates of all nuclei and electrons within the system. The total energy of the system is represented by  $E$ .<sup>[64]</sup> The Born–Oppenheimer (BO) approximation is a key tool in solving the Schrödinger equation as it simplifies the study of molecules by separating the movements of electrons and nuclei. The approximation assumes that electrons, due to their smaller mass, exhibit rapid motion compared to nuclei.<sup>[65]</sup> Therefore, by applying the BO approximation, the Schrödinger equation is solved by treating nuclei as relatively static, focusing on the electrons' movement with fixed nuclear positions.<sup>[66]</sup>

A central aspect of QM is the approximation of electron behavior by employing basis sets which are mathematical functions. The primary focus of basis sets is atomic nuclei, therefore, essential for electron modeling in molecules or solids. Furthermore, are key components for electronic structure calculations.<sup>[67]</sup> The selection of basis sets represents a critical equilibrium between

accuracy and computational expenditure, to maximize efficiency within specified computational constraints. Basis sets exhibit variability in complexity and compositional elements, incorporating diverse functional types.<sup>[68]</sup> Common basis set types include Slater-Type Orbitals (STOs), which solve the Schrödinger equation for hydrogen-like atoms and offer detailed electron interaction descriptions; Gaussian-Type Orbitals (GTOs), favored for their computational speed and ease of use in molecular calculations; and Plane Waves, ideal for describing crystals and periodic structures due to their effectiveness in periodic systems.<sup>[67]</sup>

The term “Ab Initio” originates from the Latin phrase “from the beginning” or “from first principles.” These calculations are fundamentally based on the Schrödinger equation,<sup>[69]</sup> and generate an energy value and a wavefunction when solving the Schrödinger equation for a molecule. Furthermore, the wavefunction also computes electron distribution, which is essential in assessing a molecule's polarity and identifying reactive sites for nucleophiles or electrophiles.<sup>[70]</sup> However, the Schrödinger equation is not solvable for molecules containing more than one electron and, therefore, requires the use of approximations. The extent of these approximations defines the ‘level’ of the ab initio calculation. Ab initio calculations are slower than MM, specifically with larger molecules.<sup>[71]</sup> Ab initio calculations employ various methods, with the Hartree–Fock (HF) method as the foundational technique for more advanced approaches. The principal limitation of the HF method is excluding electron correlation.<sup>[72]</sup> To enhance accuracy, post-Hartree–Fock methods are utilized, incorporating electron correlation effects. These methods include Configuration Interaction (CI), Møller–Plesset perturbation theory (MP2), and Coupled Cluster theory, all of which extend and refine the groundwork established by the Hartree–Fock method.

Semiempirical (SE) calculations similar to ab initio methods are also founded on the Schrödinger equation. However, SE calculations involve increased approximations and a precompiled library of integral values with optimized properties such as geometry or energy.<sup>[73]</sup> Parameterization is a process that incorporates experimental values into mathematical models to optimize

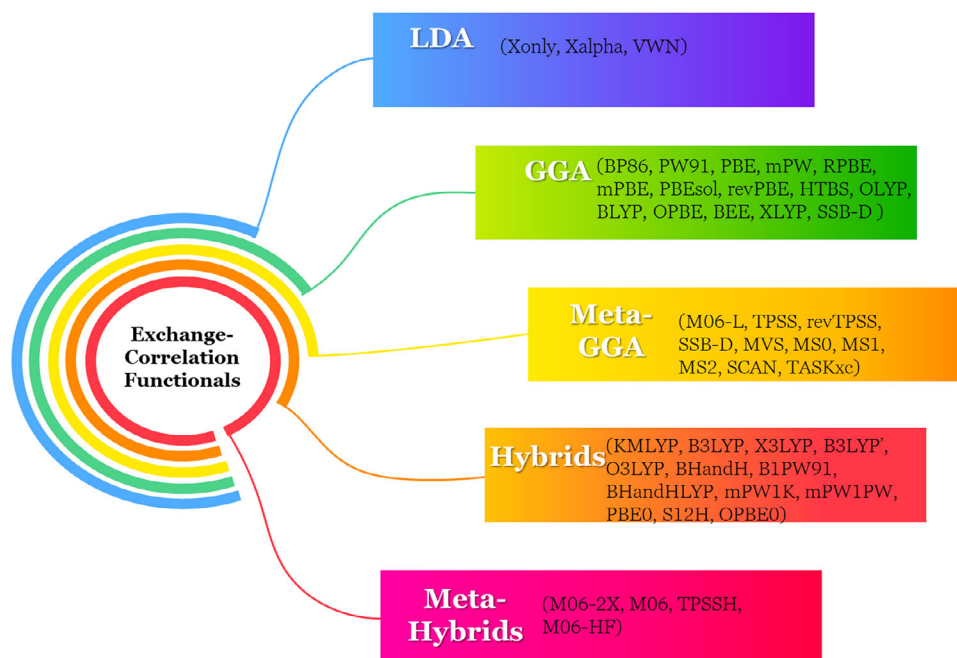


**Figure 5.** Commonly employed exchange–correlation functionals. Adapted from.<sup>[76]</sup> This is an open-access article distributed under the terms of the Creative Commons CC BY license.

calculated results. Semiempirical methods merge theoretical foundations (the Schrödinger equation) with empirical (experimental or high-level theoretical) data. Semiempirical calculations are more time-consuming than MM but significantly faster than ab initio calculations.<sup>[74]</sup>

Density Functional Theory (DFT) calculations are based on the principles of the Schrödinger equation, similar to ab initio and semiempirical approaches. However, DFT does not compute a wavefunction; instead derives an electron distribution, known as the electron density function. The computational efficiency of DFT calculations exhibits greater speed compared to ab initio methods; however, are less rapid than semiempirical approaches.<sup>[70]</sup> In DFT calculations, the Hohenberg–Kohn and Kohn–Sham theorems are employed in a complementary manner to determine the electronic properties of a system. The Hohenberg–Kohn Theorem establishes that electron density is an essential determinant of a system’s properties. Concurrently, the Kohn–Sham Theorem practically computes these properties via a system of non-interacting electrons. The main task in DFT calculations is generating accurate approximations for the exchange–correlation potential within the Kohn–Sham framework.<sup>[75]</sup>

Exchange–correlation approximations are fundamental to DFT, these approximations account for electron exchange and correlation effects in a system. In DFT, the total energy is expressed as a function of the electron density, with the exchange–correlation energy term representing electron interactions due to the Pauli exclusion principle and correlation effects.<sup>[76]</sup> Exchange–correlation functionals can generally be categorized into five main groups. (Figure 5) indicates various functionals within these groups.

**Local Density Approximation (LDA):** Assumes the exchange–correlation function at any point depends solely on the local electron density.<sup>[77]</sup>

**Generalized Gradient Approximation (GGA):** Extends LDA by incorporating density gradients, providing a more accurate electron density distribution.<sup>[78,79]</sup>

**Meta-Generalized Gradient Approximation (Meta-GGA):** An advanced exchange–correlation functional that enhances accuracy by considering additional terms beyond electron density and gradients to capture complex electronic interactions.<sup>[80,81]</sup>

**Hybrid Functionals:** Combine a GGA with a fraction of exact exchange from Hartree–Fock theory, aiming to capture both local and non-local electron correlation effects.<sup>[82]</sup>

**Meta-Hybrid Functionals:** Combine GGAs or meta-GGAs with extra components like Hartree–Fock exchange or second-order Moller–Plesset theory to balance accuracy and computational efficiency in describing electronic interactions.<sup>[80,81]</sup>

In drug design, selecting the right density functional is essential for accurately predicting molecular properties. Hybrid functionals like B3LYP are widely used due to their balanced treatment of exchange and correlation effects. Whereas meta-approximations such as M06-L excel in predicting properties like molecular excitation energies. Recent functionals like MN15 provide accuracy for both ground and excited states. Improved functionals, including M11 and M11plus, enhance accuracy for properties such as van der Waals interactions.<sup>[83]</sup> Additionally, hybrid GGAs like  $\omega$ B97X-V,  $\omega$ B97X-D3, and  $\omega$ B97X-D are effective for capturing non-covalent interactions, which is beneficial in drug design. For bioapplications, functionals that describe non-covalent interactions effectively are crucial. Recommended options include  $\omega$ B97M-V, local GGAs including

**Table 2.** Comparative analysis of molecular mechanics versus quantum mechanics methods: Advantages and disadvantages.

| Computational method    | Advantages   | Disadvantages   |
|-------------------------|--|---|
| Molecular Mechanics     | <ul style="list-style-type: none"> <li>• Computations can be efficiently conducted on personal computers with moderate specifications, broadening its accessibility across a diverse user base.</li> <li>• Integration of rapid processing, accuracy, and minimal computational requirements has established MM as a standard feature in numerous modeling software suites.</li> <li>• Generates effective initial structures as input models in computational methods including semiempirical, ab initio, or DFT calculations.</li> <li>• Can simulate extensive systems with thousands to millions of atoms, making it ideal for biological macromolecules and materials.</li> </ul> | <ul style="list-style-type: none"> <li>• Lacks the capability to provide data on the configurations and energy levels of molecular orbitals and the electronic spectra.</li> <li>• Employing an unsuitable forcefield can result in significant inaccuracies, as forcefields parameterized for specific compound classes may not exhibit reliable performance when extended to different classes of compounds.</li> <li>• Parameters are derived for ground-state systems, limiting the ability to accurately represent geometries in bond-making and bond-breaking processes.</li> </ul>     |
| Ab Initio               | <ul style="list-style-type: none"> <li>• The absence of empirical parameters in ab initio calculations, allows for application in a wide range of molecular species, including transition states and stationary points.</li> <li>• Based on QM, offer significant theoretical rigor without depending on empirical data for parameterization.</li> </ul>   | <ul style="list-style-type: none"> <li>• Calculations are resource-intensive and time-consuming, specifically for extensive systems or complex molecules. This limits the size of systems that can be feasibly investigated.</li> <li>• Requires high-end computing resources, specialized software, and expert knowledge.</li> <li>• Ab initio methods rely on approximations to make calculations feasible. These approximations can introduce errors and limitations in the results obtained.</li> <li>• Can only exactly solve the Schrödinger equation for the hydrogen atom.</li> </ul> |
| Semi-empirical          | <ul style="list-style-type: none"> <li>• Calculations are executed rapidly in comparison to ab initio and DFT, the rapid calculation time is achieved at the expense of a reduction in accuracy.</li> <li>• The generated geometries are sufficiently accurate for numerous input models that require further or more complex analyses.</li> <li>• Transition state (TS) geometries can be estimated and subsequently employed for higher-level computational analyses.</li> <li>• Generate relative energies for cations, radicals, anions, and strained molecules.</li> </ul>  | <ul style="list-style-type: none"> <li>• Unreliable results for molecules beyond the training set.</li> <li>• Parameters are prone to miscalculate steric repulsions, nucleophilicity, and basicity, resulting in inaccurate charges and molecular structures.</li> <li>• Parameters are unreliable in hydrogen bond modeling.</li> </ul>   |
| Density function theory | <ul style="list-style-type: none"> <li>• Electron correlation is incorporated, enabling DFT to determine geometries and relative energies with accuracy comparable to MP2 calculations.</li> <li>• Preferred method for geometry and energy calculations in drug design and bioapplications.</li> </ul>  | <ul style="list-style-type: none"> <li>• Requires significant computational resources, especially for large systems or high levels of theory</li> <li>• Can encounter self-interaction errors—an electron incorrectly interacts with itself, affecting predictions of ionization energies and electron affinities.</li> </ul>   |

B97-D3, revPBE-D3, and BLYP-D3, and local meta-GGAs such as B97M-rV, MS1-D3, and M06-L-D3.<sup>[84]</sup>

#### 4.3.3. Advantages and Disadvantages

The following section (Table 2) provides a comprehensive analysis of the various QM and MM methods previously highlighted, focusing on their respective advantages and disadvantages. This comparative analysis aims to provide a balanced perspective, enabling a better understanding of the strengths and limitations of each approach.<sup>[85–87]</sup>

#### 4.3.4. Previous Studies on Folate Receptor/s and Folate-Based Anticancer Drugs

A systematic review of FR research and subsequent studies on folate drug-based treatments over a decade (2014–2024) represents a focused effort to understand the interaction between FA, FRs, and the development of folate-based drugs for cancer treatment (Table 3). Employing Google Scholar as the primary database, three specific search phrases were employed to gather relevant literature: “QM analysis of folate receptors,” “MM analysis of folate receptors,” and “Computational analysis of folate-based drugs.” This search yielded a total of 29 papers. Of these, 22 papers were

**Table 3.** Computational analysis of folate receptors.

| Year | Computational aims of the study   | Classical mechanics  | Quantum mechanics | Significant findings  | Ref.  |
|------|---|--|-------------------|---|-------|
| 2014 | <ul style="list-style-type: none"> <li>Predict interactions of synthesized compounds with FR<math>\alpha</math> and FR<math>\beta</math> and glycinamide ribonucleotide formyltransferase (GARFTase).</li> <li>Analyze binding modes and interactions to understand the biological activities of the compounds.</li> <li>Assess differences in docked conformations for FR<math>\alpha</math> transport and GARFTase inhibition to identify structural requirements for selectivity and effectiveness.</li> <li>Validate the docking software for accurate prediction of compound binding modes.</li> </ul>   | <ul style="list-style-type: none"> <li>Molecular docking software (LeadIT 2.1.6)</li> <li>Ligand preparation (MOE)</li> <li>Force field (MMF94X)</li> <li>Molecular model type (Ligand–receptor complex)</li> <li>Gas phase calculation</li> </ul>   | N/A               | <ul style="list-style-type: none"> <li>Compounds 7 and 10–13 demonstrate selective inhibition toward FR <math>\alpha</math>-expressing cells, with varied effects on FR<math>\beta</math> cells.</li> <li>Compounds 7 and 11 strongly inhibit glycinamide ribonucleotide formyltransferase in KB human tumor cells, affecting purine biosynthesis.</li> <li>Demonstrated significance of <math>\alpha</math>- and <math>\gamma</math>-carboxylic acid groups, amino acid side chain length, and conformation for effective transporter binding and activity in 6-substituted pyrrolo[2,3-d]pyrimidine thienoyl antifolates.</li> <li>Potential for enhanced selective uptake through FRs suggests a pathway to targeted chemotherapy with lower toxicity.</li> <li>Provides structural insights related to the interaction between pyrrolo[2,3-d]pyrimidine scaffold and (anti)folate transporters (FR<math>\alpha</math>, FR<math>\beta</math>, PCFT, and RFC) at the L-glutamate binding site.</li> </ul> | [106] |
| 2015 | <ul style="list-style-type: none"> <li>Investigate FA's dissociation from FR<math>\alpha</math>, focusing on intermediate states, energy terms, and structural changes.</li> <li>Characterize the atomistic binding interactions between FA and FR<math>\alpha</math>, analyzing ligand and receptor conformational changes during binding.</li> <li>Validate computational results by comparing them with experimental dissociation constants and rate constants, ensuring computational analysis accuracy.</li> <li>Explore the functional effects of molecular interactions between FA and FR<math>\alpha</math> on folate-targeted drug delivery and cancer therapies involving folate uptake.</li> </ul> | <ul style="list-style-type: none"> <li>MD simulations software (GROMACS)</li> <li>Metadynamics software (PLUMED 2.0—GROMACS)</li> <li>Clustering analysis software (GROMACS)</li> <li>Force field (AMBER parm99sb)</li> <li>Solvation model (TIP3P water solvent)</li> <li>Molecular model type (Ligand–receptor complex)</li> </ul> | N/A               | <ul style="list-style-type: none"> <li>Metadynamics simulations identified intermediate states in FA's dissociation from FR<math>\alpha</math>, providing data on structural changes and the energy landscape.</li> <li>Specific residues (R103, R106, W102, W140, Y85) were crucial for FA binding, enhancing stability through stacking interactions and hydrogen bonds.</li> <li>Point mutations affected the binding affinity, with variations in dissociation constants for mutants vs the wild type, highlighting the impact of mutations on receptor functionality.</li> <li>Computational analysis offered an atomistic interpretation of experimental data, explaining variations in binding affinity due to point mutations.</li> </ul>   | [107] |

(Continued)

**Table 3.** (Continued)

| Year | Computational aims of the study   | Classical mechanics   | Quantum mechanics  | Significant findings   | Ref.  |
|------|---|---|--|--|-------|
| 2017 | <ul style="list-style-type: none"> <li>Calculate FR<math>\alpha</math> and FR<math>\beta</math> interaction structures with four compounds.</li> <li>Analyze complex properties using the density functional tight-binding method.</li> <li>Investigate intermolecular interactions with binding pocket residues.</li> <li>Understand orbital properties and frontier orbital localization in the FR pocket.</li> <li>Provide insights for designing targeted drug delivery systems based on compound interactions with FRs.</li> </ul>   | <ul style="list-style-type: none"> <li>Molecular docking software (AutoDock 4.2)</li> <li>Docking type (Flexible docking—Lamarckian algorithm)</li> <li>Gas phase calculation</li> <li>Molecular model type (ligand–receptor complex)</li> </ul>  | <p>Intermolecular interactions (SCC-DFTB-D – DFTB+ 1.2.2)</p> <p>Electron distribution (DFTB+ 1.2.2)</p> <p>Density functional tight-binding (DFTB) method</p> | <ul style="list-style-type: none"> <li>Long chains in the pterin of FA impede compound insertion, the study recommends avoiding these structures in folate derivative design.</li> <li>Compound 3 derivative exhibits higher FR<math>\alpha</math> selectivity and affinity compared to FA.</li> <li>Additional groups on the derivative enhance targeted selectivity.</li> <li>Preferred ring orientations align with the FR pocket for improved insertion.</li> <li>HOMO and LUMO analysis reveals strong interaction strengths.</li> <li>Localization of orbitals in the FR pocket underscores the importance of inserting group–pocket interactions for successful docking.</li> </ul> | [95]  |
| 2017 | <ul style="list-style-type: none"> <li>Investigate FA-PEG dendrimers' binding to FRs under physiological conditions.</li> <li>Assess the impact of PEG 750 and PEG 3350 conjugation on dendrimer–receptor interaction.</li> <li>Analyze molecular interactions, between dendrimers and the FR.</li> <li>Evaluate solubility and protection by PEG 750 and PEG 3350.</li> <li>Explore dendrimers' capabilities as drug delivery systems for cancer therapy through computational simulations.</li> </ul>                                   | <ul style="list-style-type: none"> <li>Molecular docking software (AutoDock 4.2)</li> <li>Force field (CHARMM and PARAMCHEM)</li> <li>MD simulation software (NAMD)</li> <li>Solvation model (TIP3P water boxes)</li> <li>Molecular model type (Dendrimer–folate receptor complex)</li> </ul> | <p>Dendrimer preparation (Gaussian View 5.0.9)</p>   | <ul style="list-style-type: none"> <li>PEG 750 and PEG 3350 did not affect dendrimer FR binding.</li> <li>Dendrimer folate fragments were solvent-exposed before targeting the FR.</li> <li>PEG 3350 exhibits enhanced solubility and enzymatic degradation resistance relative to PEG 750.</li> <li>Comparative analysis demonstrates a marginally enhanced affinity of FA-PEG3350 toward the FR over FA-PEG750.</li> <li>Both dendrimers are theoretically validated for use in cancer therapy drug delivery.</li> </ul>   | [108] |
| 2018 | <ul style="list-style-type: none"> <li>Determine binding energies of nine novel fluorescent antifolates (NFAs) with FR<math>\alpha</math> and FR<math>\beta</math>.</li> <li>Compare binding affinities of NFAs with those of FA for FR<math>\alpha</math> and FR<math>\beta</math> to assess NFAs' targeting potential.</li> <li>Analyze structural properties of FR-FOL and FR-NFA complexes to determine stability.</li> <li>Investigate hydrogen bond dynamics in specific FR-NFA complexes to highlight key interactions.</li> </ul> | <ul style="list-style-type: none"> <li>Molecular docking software (AutoDock 4.2)</li> <li>MD simulation software (GROMACS)</li> <li>Molecular model type (FR-NFA complex)</li> <li>Force field (AMBER99SB-ILDN)</li> <li>Solvation model (TIP3P for water)</li> </ul>                         | <p>Intermolecular interactions (SCC-DFTB-D)</p> <p>Density functional tight-binding (DFTB) method</p>  | <ul style="list-style-type: none"> <li>Compounds 4–6 with fluorescent dye exhibited higher binding energies than FR-FOL, while 7–9 (pyrazine replacements) preferred FR<math>\alpha</math>.</li> <li>Compound length influenced binding strength, with longer analogs binding more strongly.</li> <li>Compounds 7–9 demonstrated significant selectivity for FR<math>\alpha</math> based on binding energy differences.</li> <li>Molecular simulations (docking, MD, DFTB) revealed hydrogen bond insights, with MD and DFTB aligning on certain bond values.</li> </ul>   | [96]  |

(Continued)

**Table 3.** (Continued)

| Year | Computational aims of the study  | Classical mechanics  | Quantum mechanics  | Significant findings  | Ref.  |
|------|--|--|--|---|-------|
| 2018 | <ul style="list-style-type: none"> <li>Investigate binding interactions between MTX conjugates and FR<math>\alpha</math> and FR<math>\beta</math>.</li> <li>Assess the stability of MTX-FR complexes.</li> <li>Calculate binding energies between MTX and FRs.</li> <li>Compare binding energies of MTX with FR<math>\alpha</math> and RFC to evaluate receptors' relative affinities and preferences.</li> </ul>  | <ul style="list-style-type: none"> <li>Molecular docking software (AutoDock Vina)</li> <li>MD Simulation software (GROMACS)</li> <li>Force field (GROMOS 54A7)</li> <li>Solvation model (Single point charge for water molecules)</li> <li>Molecular model type (Protein-MTX conjugate)</li> </ul> | N/A  | <ul style="list-style-type: none"> <li>FR<math>\alpha</math>-positive cells showed higher MTX conjugate uptake than FR<math>\alpha</math>-negative cells, specifically for H2N-MTX-CO-FITC.</li> <li>H2N-MTX-CO-FITC uptake decreased with FA but not with calcium folinate.</li> <li>Docking and dynamics simulations indicated stable binding of the conjugate to FR<math>\alpha</math> when amino groups are oriented toward the FR<math>\alpha</math> pocket.</li> <li>Binding energy calculations showed stronger MTX and RFC complex binding than FR<math>\alpha</math>, with energies of <math>\approx 65</math> Kcal mol<math>^{-1}</math> and 15 Kcal mol<math>^{-1}</math>, respectively.</li> </ul>  | [109] |
| 2018 | <ul style="list-style-type: none"> <li>Exploring folate and its derivatives' molecular structures to understand the amide bond configuration's role in biological activity.</li> <li>Analyzing cis isomer populations along the amide bond.</li> <li>Investigating cis and trans ligand forms in saline.</li> <li>Predicting cis isomer coexistence probabilities and explaining cis form instability.</li> <li>Comparing cis and trans molecule dynamics to evaluate in vivo effects.</li> </ul>  | <ul style="list-style-type: none"> <li>MD simulation software (GROMACS)</li> <li>Force field (AMBER9929)</li> <li>Solvation model (TIP3P)</li> <li>Molecular model type (ligands)</li> </ul>   | <p>Electron density distribution (Gaussian-DFT)</p> <p>Relative energies</p> <p>NBO</p> <p>Electronic properties</p> <p>DFT functional (B3LYP)</p> | <ul style="list-style-type: none"> <li>Observed significant cis isomer presence in ligands, suggesting structural variability.</li> <li>The potential for a cis-trans equilibrium in certain ligands, indicates dynamic structural behavior.</li> <li>Cis form's energetic instability is linked to bond character changes and electron redistribution.</li> <li>Cis structures show slower dynamics than trans, affecting physiological interactions.</li> <li>Distinct shapes (Z/U for cis, V for trans) imply differences in receptor binding.</li> <li>Isomer stabilization by electrostatics and steric repulsion minimization affects molecular conformation.</li> </ul>  | [110] |
| 2018 | <ul style="list-style-type: none"> <li>Predict C7's binding mode and interactions with FR<math>\alpha</math>, identifying key binding residues.</li> <li>Model the 3D structure of peptide C7 to understand its conformation and binding affinity with FR<math>\alpha</math>.</li> <li>Analyze hydrogen bonds and H-<math>\pi</math> interactions between peptide C7 and FR<math>\alpha</math>, to understand the binding mechanism.</li> <li>Compare C7's binding mode with FR<math>\alpha</math> to folate's, assessing similarities and differences to ascertain C7's targeting potential.</li> </ul> | <ul style="list-style-type: none"> <li>Molecular docking software (ClusPro)</li> <li>MD simulation software (GROMACS)</li> <li>Molecular model type (peptide-protein complex)</li> </ul>   | N/A  | <ul style="list-style-type: none"> <li>C7 binds near FR<math>\alpha</math>'s folate-binding pocket entrance, engaging in key interactions including hydrogen bonds and H-<math>\pi</math> interactions with FR<math>\alpha</math> residues.</li> <li>Predicted 3D structure reveals C7 in a random coil configuration, enhancing its binding flexibility with FR<math>\alpha</math>.</li> <li>Identified specific interactions between C7 and FR<math>\alpha</math>, notably hydrogen bonds with Tyr60, Ser101, Trp138, and H-<math>\pi</math> interactions with Trp140, crucial for complex stability and binding affinity.</li> <li>Compared C7's surface binding near the folate pocket entrance to folate's deeper docking, suggesting C7's unique, though relatively weaker, affinity.</li> <li>Highlighted C7's potential for FR<math>\alpha</math>-specific targeting, based on a unique hydrogen bond with R61, suggesting enhanced specificity for tumor cells with reduced off-target effects.</li> </ul> | [111] |

(Continued)

**Table 3.** (Continued)

| Year | Computational aims of the study   | Classical mechanics  | Quantum mechanics   | Significant findings   | Ref.  |
|------|---|--|---|--|-------|
| 2019 | <ul style="list-style-type: none"> <li>Explore FA's conformational flexibility by analyzing 60 conformers and focusing on the three most stable for in-depth study.</li> <li>Understand the electronic structure of FA conformers.</li> <li>Simulate valence photoelectron spectra of FA conformers.</li> <li>Calculate and compare the vertical ionization energies of FA conformers with experimental data to validate computational approaches.</li> <li>Investigate how conformational changes affect FA's bioactivity, ligand–receptor binding, and protein interactions.</li> </ul> | N/A  | <p>Conformer optimization (Gaussian—DFT)</p> <p>Ionization energy (Gaussian)</p> <p>NBO (Gaussian)</p> <p>DFT functional (B3LYP and M06-2X)</p> | <ul style="list-style-type: none"> <li>Identified three most stable gas-phase conformers of FA, highlighting structural flexibility.</li> <li>Electronic structure analysis showed lowest energy ionizations primarily arise from the p-aminobenzoyl moiety.</li> <li>Calculated vertical ionization energies for FA conformers, noting differences between conformers and in protein-bound states.</li> <li>Bioactive FA conformers show a <math>\approx 0.5</math> eV increase in HOMO ionization energies compared to stable free conformers.</li> <li>Observed a link between hydrogen bond strength and increased ionization energies in MOs with nitrogen or oxygen lone pairs.</li> </ul>   | [112] |
| 2019 | <ul style="list-style-type: none"> <li>Describing folate and antifolates under physiological conditions.</li> <li>Obtain insights into folate and its analogs in solution via atomistic molecular dynamics simulations.</li> <li>Investigate molecular characteristics of ligands.</li> </ul>   | <ul style="list-style-type: none"> <li>Molecular docking software (AutoDock Vina)</li> <li>MD simulation software (GROMACS)</li> <li>Force field (AMBER84)</li> <li>Solvation model (TIP3P)</li> <li>Molecular model type (ligand–receptor complex)</li> </ul>             | <p>Single point calculations (Gaussian -DFT)</p> <p>NBO (Gaussian)</p> <p>DFT functional (B3LYP)</p>  | <ul style="list-style-type: none"> <li>Modelled two folates and four antifolates in saline.</li> <li>Identified high flexibility and distinct U-, Z-, or quasi-linear conformations.</li> <li>Chemical structure changes led to localized electron density shifts.</li> <li>Pterin and terminal amino acids are critical for structure; the central part is less influential.</li> <li>Ligands showed flexibility, with specific pterin and terminal fragment conformations.</li> <li>U-, Z-shape, or quasi-linear structures noted, with amino acid orientation variations.</li> <li>Intramolecular hydrogen bonds affected flexibility and conformation.</li> <li>Despite structural variations, the interaction area with water remained relatively constant.</li> <li>Similar water interactions, but differences in backbone conformations, shape, and electron density were observed.</li> </ul> | [113] |
| 2019 | <ul style="list-style-type: none"> <li>Create twenty new compounds with varied functional groups (—COOH, —OH, —NH<sub>2</sub>, —CH<sub>3</sub>) to explore interactions with FRs.</li> <li>Investigate compound–receptor binding.</li> <li>Assess the influence of functional groups on complex stability.</li> <li>Examine interactions between compounds and FRs, highlighting the role of hydroxyl, carboxyl, and amino groups.</li> <li>Propose design strategies for potent folate receptor-targeted compounds based on binding models.</li> </ul>                                   | <ul style="list-style-type: none"> <li>Molecular docking software (AutoDock)</li> <li>MD simulation software (GROMACS)</li> <li>Force field (Amber99sb-ildn)</li> <li>Solvation model (TIP3P for water)</li> <li>Molecular model type (ligand–receptor complex)</li> </ul> | N/A   | <ul style="list-style-type: none"> <li>Docking predicted similar binding poses for four ligands in the folate receptor-<math>\alpha</math>'s active site, with structural adjustments from saline to receptor binding.</li> <li>Functional group introduction increases compound dipole moments and binding energies in the order: —OH &gt; —CH<sub>3</sub> &gt; —COOH.</li> <li>MD simulations show hydrogen bond conservation in pterin moiety; glutamate moiety's hydrogen bonds shift to water molecules.</li> <li>RMSD values below 0.25 nm indicate equilibrium in all complexes.</li> <li>Minor fluctuations in FR docking pocket residues, larger fluctuations in residues interacting with the glutamate moiety.</li> <li>OH group links more stably to the compound compared to other groups.</li> </ul>   | [114] |

(Continued)

**Table 3.** (Continued)

| Year | Computational aims of the study  | Classical mechanics  | Quantum mechanics   | Significant findings   | Ref.  |
|------|--|--|---|--|-------|
| 2019 | <ul style="list-style-type: none"> <li>Identify the most stable tautomeric forms of FA</li> <li>Use atomistic molecular dynamics simulations to observe FA tautomers in saline.</li> <li>Investigate the influence of molecular conformation on the energy hierarchy of tautomers.</li> <li>Predict FA tautomers' interactions with the FR via flexible docking.</li> <li>Calculate NMR chemical shifts of FA tautomers in water and DMSO with computational models.</li> </ul>  | <ul style="list-style-type: none"> <li>Molecular docking software (AutoDock Vina)</li> <li>MD simulation software (GROMACS)</li> <li>Force field (AMBER9929)</li> <li>Solvation model (TIP3P)</li> <li>Molecular model type (ligand–receptor complex)</li> </ul> | <p>Geometry optimization (Gaussian)</p> <p>NBO (Gaussian)</p> <p>NMR (Gaussian)</p> <p>-PCM</p> <p>DFT functional (B3LYP)</p> | <ul style="list-style-type: none"> <li>The lactam FA-N3 tautomer of FA is the most energy-efficient, with FA-N1 being 2.5 kcal mol<sup>-1</sup> higher.</li> <li>Both lactam tautomers exhibit similar saline interactions, suggesting comparable FR interactions.</li> <li><sup>1</sup>H NMR spectra confirm lactam tautomers in water and DMSO, with rapid proton exchange at N1 and N3 of pterin.</li> <li>Tautomers' energy ordering remains unchanged by the molecule's conformation.</li> <li>Combines theoretical and experimental NMR data to clarify folate's predominant tautomeric form in solution.</li> </ul>   | [115] |
| 2020 | <ul style="list-style-type: none"> <li>Develop a multilipid bilayer model with FR-<math>\alpha</math> to study folate-based drug delivery systems.</li> <li>Explore FR and membrane behavior under various pressure scaling schemes, focusing on volume fluctuations and structural changes.</li> <li>Analyze density profiles, lipid area, and deuterium order parameters to understand the model neoplastic cell membrane properties.</li> <li>Examine interactions and dynamics of membrane-anchored protein receptors, especially FR-<math>\alpha</math>, to enhance understanding of drug delivery targeting cancer cells.</li> </ul> | <ul style="list-style-type: none"> <li>Force field (CHARMM36)</li> <li>MD simulation software (GROMACS)</li> <li>Membrane analysis (APL@Voro) Molecular model type (ligand–receptor complex)</li> <li>Solvation model (TIP3P)</li> </ul>                         | N/A   | <ul style="list-style-type: none"> <li>Semi-isotropic pressure scaling significantly impacts FR and membrane behavior.</li> <li>Ligand binding pocket volume exhibits “waving” motions, indicating protein movement toward and away from the membrane, distinct from major structural alterations.</li> <li>Simulations with constant nonzero surface tension most closely mirror experimental data, underscoring its importance in accurate system modeling.</li> <li>A multilipid bilayer model incorporating GPI-anchored FR-<math>\alpha</math> provides insights into receptor dynamics in a physiological context, crucial for developing folate-based drug delivery methods.</li> <li>The study highlights the intricate interactions between FR-<math>\alpha</math> and the membrane, contributing to enhanced drug delivery approaches for cancer therapy.</li> </ul> | [116] |
| 2020 | <ul style="list-style-type: none"> <li>Investigate FA-Myr-BSA nanoparticles (NPs) binding to FRs to elucidate their cancer cell targeting mechanisms.</li> <li>Employ DFT calculations to examine myricetin's electronic structure, including HOMO and LUMO energies, for chemical property insights.</li> <li>Computationally confirm the binding affinity and interactions of NPs with the FRs, supporting experimental findings and clarifying the action mechanism at the molecular level.</li> </ul>  | <ul style="list-style-type: none"> <li>Molecular docking software (Schrodinger—GLIDE)</li> <li>Force field (OPLS4)</li> <li>Molecular model type (ligand–receptor complex)</li> <li>Solvation model (TIP3P)</li> </ul>   | <p>Geometry optimization (Gaussian—DFT)</p> <p>Molecular orbital energies (Gaussian)</p> <p>DFT functional (B3LYP)</p>        | <ul style="list-style-type: none"> <li>Molecular docking confirmed FA-Myr-BSA NPs' affinity for FRs, promoting active endocytosis.</li> <li>Myr exhibited an elevated energy band gap, contributing to its enhanced biological activity.</li> <li>Myr in BSA NPs binds to the FR binding site through weak non-covalent interactions.</li> <li>Docking analysis demonstrates FA-Myr-BSA NPs can bind to FR on cancer cell surfaces, promoting endocytosis.</li> </ul>  | [117] |

(Continued)

**Table 3.** (Continued)

| Year | Computational aims of the study   | Classical mechanics   | Quantum mechanics  | Significant findings  | Ref.  |
|------|---|---|--|---|-------|
| 2020 | <ul style="list-style-type: none"> <li>Analyze functional group effects (methyl, carboxyl, hydroxyl, amino) on FR<math>\alpha</math> and <math>\beta</math> binding.</li> <li>Assess the impact of functional group size on binding affinity with FR<math>\alpha</math> and <math>\beta</math>.</li> <li>Design targeted antifolates for specific FR subtypes to enhance therapeutic/imaging agent delivery.</li> <li>Improve specificity of folate-targeted probes by modifying FA and its coupling compounds for enhanced FR <math>\alpha</math> and <math>\beta</math> targeting efficiency.</li> </ul>  | <ul style="list-style-type: none"> <li>Molecular docking software (AutoDock)</li> <li>MD simulation software (GROMACS)</li> <li>Force field (Amber99sb-ildn)</li> <li>Solvation model (TIP3P)</li> </ul>  | Structure optimization (DFTB-D)  | <ul style="list-style-type: none"> <li>Functional groups (methyl, carboxyl, hydroxyl, amino) significantly influence complex stabilization with FR<math>\alpha</math> and <math>\beta</math>.</li> <li>Hydroxyl groups enhance stability more than other groups in receptor interactions.</li> <li>Longer functional groups improve binding affinity with receptor <math>\alpha</math> but reduce it with receptor <math>\beta</math>.</li> <li>Compounds mimic folate binding, with pterate in the negatively charged pocket and glutamate outside.</li> <li>FR <math>\beta</math>'s smaller pocket leads to weaker compound interactions compared to FR <math>\alpha</math>.</li> </ul>                     | [97]  |
| 2020 | <ul style="list-style-type: none"> <li>Confirm (2E)-3-(biphenyl-4-yl)-1-(4-bromophenyl)prop-2-en-1-one molecular structure using spectroscopic methods.</li> <li>Determine the stability and optimal conformation of 3BPO.</li> <li>Examine the structural properties of 3BPO in various solvents to understand its behavior in solvent-phase environments.</li> <li>Conduct a comparative analysis of FT-IR and FT-Raman spectra to identify functional groups and analyze the Potential Energy Distribution (PED) for vibrational energies.</li> <li>Investigate electronic transitions and molecular reactivity of 3BPO.</li> <li>Identify reactive sites within 3BPO to predict interactions with biological targets.</li> <li>Elucidate the interaction mechanism between 3BPO and the FR<math>\alpha</math> bound to FA.</li> </ul> | <ul style="list-style-type: none"> <li>Molecular docking software (AutoDock)</li> <li>Molecular model type (ligand–receptor complex)</li> </ul>   | PES scan<br>Geometry optimization<br>Vibrational assignments<br>(VEDA4)<br>Molecular orbital energies<br>UV–vis<br>Molecular electrostatic potential<br>Hyperpolarizability<br>Thermodynamics<br>NBO<br>DFT functional (B3LYP and M062X) | <ul style="list-style-type: none"> <li>Demonstrated high congruence between experimental and theoretical bond lengths and angles, highlighting strong C–H bond characteristics.</li> <li>Computed static thermodynamic functions across temperatures (100–1000 K), observing an increase in functions with temperature.</li> <li>Investigated nonlinear optical properties, comparing the compound's NLO values to standards like Urea across different solvents, noting higher hyperpolarizability in water and DMSO.</li> </ul>   | [118] |
| 2021 | <ul style="list-style-type: none"> <li>Study the binding affinity and stability of FA conjugated to <math>\beta</math>CD vs unconjugated FA and ligand-free systems toward FR<math>\alpha</math>.</li> <li>Analyze FA-<math>\beta</math>CD/FR<math>\alpha</math> interactions and dynamics.</li> <li>Examine the impact of <math>\beta</math>CD conjugation on the stability, mobility, and energy of the FR<math>\alpha</math> binding site.</li> <li>Investigate the potential of FA-<math>\beta</math>CD conjugation for targeted cancer therapy delivery.</li> <li>Explore how <math>\beta</math>CD conjugation enhances the efficacy and stability of drug–receptor interactions in targeted therapies.</li> </ul>   | <ul style="list-style-type: none"> <li>Molecular docking software (AutoDock)</li> <li>MD simulation software (AMBER 18)</li> <li>Force field (AMBER ff14SB)</li> <li>Molecular model type (ligand–receptor complex)</li> <li>Solvation model (TIP3P)</li> </ul> | N/A  | <ul style="list-style-type: none"> <li>Docking demonstrated high binding affinity between conjugated FA and FR<math>\alpha</math>.</li> <li>MD simulations confirmed higher stability of the FA-<math>\beta</math>CD/FR<math>\alpha</math> system vs unconjugated FA and apo-FR<math>\alpha</math>.</li> <li>Equilibrium was achieved with stable RMSD and Rg values, indicating system consistency.</li> <li><math>\beta</math>CD conjugation enhanced stability and reduced residue mobility at the FR<math>\alpha</math> binding site.</li> <li>Analysis identified residues contributing favorably to energy and stability, underscoring the conjugate's potential for targeted drug delivery.</li> </ul> | [119] |

(Continued)

**Table 3.** (Continued)

| Year | Computational aims of the study   | Classical mechanics  | Quantum mechanics | Significant findings  | Ref.  |
|------|---|--|-------------------|---|-------|
| 2021 | <ul style="list-style-type: none"> <li>Investigate the effects of heterocyclic substitutions on FA's affinity and stability with FR<math>\alpha</math>.</li> <li>Analyze molecular interactions between heterocyclic-substituted FA derivatives and FR<math>\alpha</math>.</li> <li>Assess the therapeutic potential of these derivatives for FR<math>\alpha</math>-targeted treatments.</li> <li>Advanced understanding of structure–activity relationships in FR<math>\alpha</math> ligand design.</li> </ul>   | <ul style="list-style-type: none"> <li>Molecular docking software (AutoDock)</li> <li>MD simulation software (AMBER)</li> <li>Force field (AMBER ff14SB)</li> <li>Molecular model type (ligand–receptor complex)</li> <li>Solvation model (TIP3P)</li> </ul>     | N/A               | <ul style="list-style-type: none"> <li>Tetrazole (FOL3) and benzothioephene (FOL08) substitutions enhance FA analogs' affinity for FR<math>\alpha</math>.</li> <li>FA analogs FOL03 and FOL08 exhibit strong binding and interactions with FR<math>\alpha</math>'s active site.</li> <li>Molecular docking and dynamics simulations confirm stable complexes between these analogs and FR<math>\alpha</math>.</li> <li>These substitutions increase electrostatic attractions within the FR<math>\alpha</math> binding pocket.</li> <li>ADMETox predictions favor FOL03 and FOL08 as lead candidates for cancer therapy.</li> </ul>   | [120] |
| 2021 | <ul style="list-style-type: none"> <li>Investigate the binding of two folate forms and four derivatives to FR-<math>\alpha</math> using all-atom MD simulations under physiological conditions.</li> <li>Evaluate the specificity of the ligands and elucidate the intermolecular interactions during the binding process to FR-<math>\alpha</math>.</li> <li>Study ligand–receptor interactions, focusing on the receptor embedded in a cell membrane, in physiological environments.</li> <li>Provide insights into designing FR-<math>\alpha</math>-targeted drug delivery systems through a detailed understanding of ligand specificity and affinity.</li> <li>Analyze the initial spontaneous binding stages of folate and its derivatives to FR-<math>\alpha</math>, aiming to improve targeted drug delivery system development.</li> </ul> | <ul style="list-style-type: none"> <li>Force field (CHARMM)</li> <li>MD simulation software (GROMACS)</li> <li>Solvation model (TIP3P)</li> <li>Molecular model type (ligand–receptor complex)</li> </ul>  | N/A               | <ul style="list-style-type: none"> <li>Simulations revealed spontaneous binding of all molecules within nanoseconds, showing variation in binding time, location, and duration across different ligands.</li> <li>Folate, 5-methyltetrahydrofolate, and rilritrexed exhibited specific binding to the active site of the receptor, while pemetrexed displayed nonspecific binding. Methotrexate and pteroyornithine demonstrated weaker binding affinities.</li> <li>Two binding poses were identified, with one aligning with the crystal structure of the folate-FR<math>\alpha</math> complex, confirming the simulation's accuracy in replicating experimental binding configurations.</li> <li>Ligand–receptor binding to the active site was characterized by hydrogen bonds, <math>\pi</math>-stacking, and van der Waals and Coulomb interactions, highlighting mechanisms critical for effective binding.</li> <li>The computational approach was validated by the simulations' ability to reproduce results with limited trajectories, consistent with experimental binding affinity data.</li> </ul> | [121] |
| 2022 | <ul style="list-style-type: none"> <li>Investigate structures and binding affinities of eight novel antifolates with FR<math>\alpha</math> and FR<math>\beta</math>.</li> <li>Compare binding energies between FR<math>\alpha</math> and FR<math>\beta</math> for these antifolates.</li> <li>Analyze binding structures, interaction residues, pocket volume, and surface area of complexes.</li> <li>Examine root mean square displacement and secondary structural elements of bound complexes through MD simulations.</li> <li>Design targeted antifolates for FR<math>\alpha</math> and FR<math>\beta</math> to differentiate between cancer cells and inflammation.</li> </ul>  | <ul style="list-style-type: none"> <li>Molecular docking software (AutoDock)</li> <li>MD simulation software (GROMACS)</li> <li>Force field (AMBER99SB-ILDN)</li> <li>Solvation model (TIP3P)</li> <li>Molecular model type (ligand–receptor complex)</li> </ul> | N/A               | <ul style="list-style-type: none"> <li>Compounds 3 and 8 showed distinct binding energies to FR<math>\alpha</math> and FR<math>\beta</math>, highlighting their potential for FR<math>\alpha</math>-targeted drug delivery.</li> <li>Insight into the complexes' molecular interactions was gained through analysis of binding structures, interaction residues, pocket volume, and surface area.</li> <li>Stability in root mean square displacement and secondary structural elements indicated equilibrium in the bound complexes.</li> </ul>  | [122] |

(Continued)

**Table 3.** (Continued)

| Year | Computational aims of the study   | Classical mechanics   | Quantum mechanics   | Significant findings   | Ref.  |
|------|---|---|---|--|-------|
| 2022 | <ul style="list-style-type: none"> <li>Conduct MD simulations to elucidate the binding dynamics of FA and the FA-PEG-5-FU pro-drug with FR<math>\alpha</math>.</li> <li>Investigate the stability of FA and FA-PEG-5-FU within the FR<math>\alpha</math> active site using computational methods.</li> <li>Analyze the contribution of specific amino acids, including Trp138, Trp140, and Lys136, to the stabilization of the flexible loop adjacent to the FR<math>\alpha</math> active site.</li> <li>Utilize MD simulations to explore the binding modes of FA and FA-PEG-5-FU with FR<math>\alpha</math> and their implications for targeted drug delivery.</li> </ul> | <ul style="list-style-type: none"> <li>Molecular docking software (AutoDock)</li> <li>MD simulation software (AMBER)</li> <li>Force field (AMBERff99SB)</li> <li>Solvation model (TIP3P)</li> <li>Molecular model type (ligand–receptor complex)</li> </ul> | N/A   | <ul style="list-style-type: none"> <li>MD simulations indicated that the FA-PEG-5-FU prodrug complex has higher stability and binding affinity with FR<math>\alpha</math> than FA alone.</li> <li>Interaction analysis between amino acids and the FA-PEG-5-FU prodrug complex with FR<math>\alpha</math> identified specific residues (Trp138, Trp140, and Lys136) that stabilize the active site's flexible loop, improving drug binding.</li> <li>The FA-PEG-5-FU complex showed less flexibility upstream compared to the crystallized FA/FR<math>\alpha</math> complex, suggesting a more stable binding configuration.</li> </ul>  | [123] |
| 2022 | <ul style="list-style-type: none"> <li>Compare the antioxidant properties of four antifolates to FA.</li> <li>Calculate N–H bond dissociation energy and vertical ionization potential in water.</li> <li>Analyze the stability of radicals and radical cations from folate and antifolate molecules.</li> <li>Conduct MD simulations for conformational stability insights.</li> <li>Examine conformational behavior, hydrogen bonding, RMSD, SASA, and cluster structures of molecules</li> </ul>   | <ul style="list-style-type: none"> <li>MD simulation software (AMBER)</li> <li>Force field (GAFF)</li> <li>Solvation model (TIP3P)</li> <li>Molecular model type (ligand–receptor complex)</li> </ul>   | <p>Geometry optimization</p> <p>Single-point energy calculation</p> <p>Solvent effects</p> <p>NBO (Gaussian)</p> <p>DFT functional (wb97XD)</p> | <ul style="list-style-type: none"> <li>N–H bond dissociation energy and vertical ionization potential for antifolate molecules demonstrate similar antioxidant properties to FA.</li> <li>Tautomeric analysis reveals stable configurations for the pterin and 2,4-diaminopteridin sections with distinct energy rankings.</li> <li>MD simulations demonstrate antifolates' significant flexibility and varied conformations in water, similar to FA.</li> <li>RMSD values reveal minor structural differences from FA, suggesting subtle molecular modifications slightly affect their properties.</li> <li>Antifolates largely mimic FA's behavior under physiological conditions, despite minor modifications to their molecular structure.</li> </ul>      | [124] |
| 2022 | <ul style="list-style-type: none"> <li>Explore the binding effects of acidic pH cancer cells between FA and FR<math>\alpha</math>.</li> <li>Examine the interaction between FR<math>\alpha</math> ionizable residues' protonation states and FA.</li> <li>Analyze pH-induced stability and conformational changes in the FA–FR<math>\alpha</math> complex through MD simulations.</li> <li>Aim to enhance cancer diagnostics and therapy by understanding the impact of pH on FA–FR<math>\alpha</math> interaction.</li> </ul>  | <ul style="list-style-type: none"> <li>MD simulation software (AMBER)</li> <li>Force fields (ff14SB and GAFF)</li> <li>Molecular model type (ligand–receptor complex)</li> </ul>  | N/A   | <ul style="list-style-type: none"> <li>FA exhibits a 50-fold higher binding affinity to FR<math>\alpha</math> compared to FRB.</li> <li>At acidic pH, FA's affinity for FR<math>\alpha</math> drops dramatically (by 2000-fold) compared to physiological pH, affecting interaction stability.</li> <li>MD simulations identified changes in protonation states of FR<math>\alpha</math>'s residues and their effects on FA's binding within its ligand site.</li> <li>Protonation of Asp81 in FR<math>\alpha</math>'s binding site releases FA's pterin ring, impairing binding.</li> <li>Gd-DTPA-folate's interaction with FRA is predicted to be more stable at low pH, suggesting a new avenue for creating selective cancer diagnostic agents.</li> </ul> | [125] |

deemed directly relevant to the study's objectives and were therefore selected for comprehensive analysis. The selection criteria ensured a focused review on the utilization of QM and MM analysis methods, to deepen the understanding of how FA can be used effectively in cancer therapeutics.

In recent years, molecular docking has evolved into a crucial instrument for in-silico drug design and development within the framework of classical mechanics approaches.<sup>[88]</sup> This technique models interactions at an atomic level, specifically between small molecules and a protein of interest. This results in the behavior characterization of small molecules when within the binding site of a target protein.<sup>[89]</sup> A wide array of computational tools are available for molecular docking methods, including both proprietary and open-source options.<sup>[90]</sup> A previous study indicates that the most frequently utilized software applications for molecular docking are AutoDock Vina, Discovery Studio, Surflex, AutoDock GOLD, Glide, MCDock, MOE-Dock, FlexX, DOCK, LeDock, rDock, ICM, Cdcker, LigandFit, FRED, and UCSF Dock.<sup>[91]</sup> However, AutoDock Vina, Glide, and AutoDock GOLD have been identified as the leading options, as they demonstrate accurate docking scores.<sup>[88]</sup> The systematic review analysis of docking tools indicates 13 studies employed AutoDock or AutoDock Vina and two studies, which correlates with the findings of Agu et al.<sup>[88]</sup>

Molecular dynamics simulations are extensively employed to explore conformational changes during the interactions between proteins and macromolecular complexes, providing an understanding of basic functions, operational principles, and mechanisms at the molecular level.<sup>[92]</sup> There are several software packages available for MD simulations which include, CHARMM, GROMACS, NAMD, AMBER, and OpenMM.<sup>[93]</sup> Literature indicates that GROMACS is a preferred option for MD simulations, especially in protein studies. Key advantages of GROMACS include speed, accuracy, and adaptability in conducting high-speed biomolecular simulations.<sup>[94]</sup> The systematic review of MD simulations reveals that GROMACS is the most commonly used software in FR research, with 12 studies utilizing it, followed by AMBER with five studies.

Table 3 indicates several studies that have included the self-consistent charge density functional tight-binding (SCC-DFTB) approach.<sup>[95–97]</sup> This approximates QM derived from DFT and uses a second-order expansion of the DFT total energy expression. It aims to overcome the limitations of conventional DFT methods in accurately modeling biological systems, especially in scenarios involving weak binding forces and charge transfer problems.<sup>[98]</sup>

Furthermore, in all studies that have QM calculations, GTOs were employed. In biological research, GTOs are prevalently employed for the electronic structure calculations of biomolecules, with the 6–31G(d) basis set being predominantly used. This set, distinguished by the inclusion of polarization functions (d functions) on heavy atoms, enhances the accuracy of electronic structure descriptions for molecules comprising elements like carbon, nitrogen, oxygen, and sulfur. In addition, this basis set balances detailed molecular insight and computational manageability; therefore, is preferred in the study of biomolecular electronic structures.<sup>[67]</sup>

The progression of research on FR interactions from 2014 to 2023 highlights a significant evolution in strategies for cancer

therapy, particularly in the context of targeted drug delivery systems. Early research from 2014 to 2016 established the foundation by focusing on the prediction of interactions with synthesized compounds, analyzing binding modes, and understanding the structural requirements for effective and selective drug delivery systems targeting FRs. In 2014, the research aimed to predict interactions with FRs (FR $\alpha$ , FR $\beta$ ) and glycinamide ribonucleotide formyltransferase (GARFTase), analyze binding modes, and validate docking software. The study identified selective inhibition by specific compounds and highlighted structural features crucial for binding and activity, suggesting pathways for targeted chemotherapy with lower toxicity. However, the reliance on classical mechanics without quantum mechanical validations limited the study's scope. By 2015, the focus shifted to investigating FA's dissociation from FR $\alpha$  and characterizing atomistic interactions using MD simulations and metadynamics. Key residues and intermediate states were identified, enhancing the understanding of dynamic binding processes and receptor functionality. This study provided a deeper insight into receptor–ligand interactions but was focused primarily on FA dissociation, limiting its broader therapeutic implications.

In the following years (2017–2018), research efforts concentrated on analyzing interaction structures and intermolecular interactions. The first study in 2017 employed density functional tight-binding (DFTB) methods to calculate interaction structures with FR $\alpha$  and FR $\beta$  and analyze intermolecular interactions. The study provided valuable insights into structural features and binding modes. However, being purely theoretical, its direct application to drug design is limited. The second study in 2017 assessed the binding of FA-PEG dendrimers to FRs, demonstrating enhanced solubility and stability, and potential for cancer therapy. These findings highlighted practical implications for drug delivery systems, yet in vivo studies were needed for further validation. In 2018, the first study focused on determining the binding energies of novel fluorescent antifolates (NFAs) with FR $\alpha$  and FR $\beta$  using molecular docking and dynamics simulations. The study identified higher binding energies for NFAs with specific structural properties and provided insights into hydrogen bond dynamics, aiding in the design of targeted antifolates. However, the impact of fluorescent properties on biological systems was not fully explored. The second study in 2018 investigated MTX conjugates' binding to FR $\alpha$  and FR $\beta$ , highlighting the importance of amino group orientation for binding stability and suggesting pathways for further drug development targeting FR $\alpha$ . By 2019 and 2020, the scope of research expanded to examine the conformational flexibility of folate derivatives and the influence of functional groups on the stability of these complexes, alongside the development of multilipid bilayer models for fine-tuning drug targeting mechanisms. In 2019, the first study explored FA conformational flexibility and electronic structure using DFT and MD simulations, identifying stable conformers and ionization energies. The study provided detailed insights into FA conformers; however, didn't entirely address practical applications in therapeutic contexts. The second study in 2019 investigated folate and antifolates in solution, revealing structural flexibility and consistent interactions with water. While this study advanced the understanding of the dynamic nature of these molecules, its broader implications for drug design and delivery required further exploration. In 2020, the first study developed a multilipid bilayer

model to study folate-based drug delivery systems, providing insights into a receptor–membrane interactions crucial for developing effective drug delivery systems. The second study in 2020 investigated the binding of FA-Myr-BSA NPs to FRs, demonstrating the potential for cancer cell targeting and enhanced biological activity. However, in vivo validations were necessary to confirm these findings.

This period marked a shift toward a more nuanced investigation of molecular structures and interactions to refine cancer therapy approaches. Alongside these developments, computational methods also saw parallel improvements. The transition from basic molecular docking to complex MD simulations and QM calculations illustrates a broader trend toward leveraging enhanced computational techniques for detailed insights. The research increasingly focused on the specificity and selectivity of folate-based drugs, aiming to minimize off-target effects and enhance therapeutic efficacy.

Furthermore, the exploration of novel drug candidates and targeted delivery systems reflects an ongoing pursuit of innovative solutions in drug development. This is observed from 2021 to 2023, when studies demonstrated the enhanced binding affinity and stability of  $\beta$ -cyclodextrin ( $\beta$ CD) conjugated with FA to FR $\alpha$ , signifying a leap in potential for targeted drug delivery. The research highlighted the promise of heterocyclic substitutions on FA for increasing affinity toward FR $\alpha$ , and detailed MD simulations provided key insights into spontaneous binding mechanisms of folate forms and derivatives. Investigations into novel antifolates in 2022 revealed distinct binding energies to FR $\alpha$  and FR $\beta$ , demonstrating their potential for precision drug delivery. Additionally, research on FA-PEG-5-FU prodrug complexes emphasized the role of specific amino acids in enhancing drug–receptor complex stability.

#### 4.3.5. Future Directions

*Dynamic Behavior under Physiological Conditions:* Studies frequently concentrate on static binding interactions, often neglecting the dynamic behavior of ligand–receptor complexes under physiological conditions. The 2022 study on pH effects represents progress in this area; however, further research is required to comprehensively understand the behavior of these complexes across diverse physiological environments.

*Broader Range of Ligands:* Most studies concentrate on a limited set of folate derivatives and antifolates. Exploring a broader range of ligands, including those with novel functional groups or backbones, could uncover new insights into FR interactions and potential therapeutic applications.

*Synergistic Effects with Other Therapies:* Most studies focus on folate or its derivatives in isolation. Investigating the interaction mechanisms between these compounds in combination with other therapeutic agents or within multi-drug regimens could offer valuable insights for developing comprehensive cancer treatment strategies.

*Integration of Computational Models:* In the field of drug delivery, an array of simulation methodologies can be implemented. The Monte Carlo (MC) simulation uses stochastic sampling and generates numerous potential outcomes in complex systems.<sup>[99]</sup> It is instrumental in drug delivery systems (DDSs) for simulat-

ing drug and delivery vehicle behaviors, aiding in the optimization of drug delivery strategies.<sup>[100]</sup> Both Finite Element Analysis (FEA) and Computational Fluid Dynamics (CFD) can be employed to simulate the translocation of a pharmaceutical agent through a biological system. The FEA is suited to complex systems, as it divides the system into smaller segments for individual analysis.<sup>[101]</sup> Conversely, CFD operates through the use of numerical algorithms.<sup>[102]</sup>

Currently, MD, MC, FEA, and CFD are used independently in DDS simulations. Combining two or more of these methods can enhance the understanding of DDS by leveraging the strengths of individual approaches as a collective.

There are two integration modeling strategies. The first is a multiscale model that integrates different models across varied time and length ranges, which necessitates optimization and validation to achieve coherence with data outputs. Despite its complexity, this framework is a robust tool for advancing drug delivery technologies and improving therapeutic outcomes.<sup>[103]</sup> The second strategy is a hybrid model, which combines multiple simulation techniques to model different aspects of DDS behavior. Hybrid models are more resource-efficient than multiscale models, as no data exchange between different ranges is required.

Artificial intelligence (AI) and machine learning (ML) hold significant potential for advancing the field of drug delivery. These technologies process extensive datasets from simulation models, identifying and connecting patterns, where traditional statistical methods fail.<sup>[104,105]</sup>

*Advancing Scientific Research through Open-Source Platforms and Collaborative Practices:* Open-source software platforms, serve as a universal infrastructure for the development and distribution of simulation models. The dissemination of simulation data and models, coupled with data sharing and collaboration among researchers, significantly enhances the accuracy and reproducibility of these models. These practices foster transparency, stimulate innovation, and contribute to the advancement of scientific research.

## 5. Conclusion

The process of pharmaceutical development, from concept to market, is both protracted and financially burdensome. The integration of computational chemistry into this landscape has accelerated the development process by employing drug efficacy and safety profile assessments. Central to drug action mechanisms is the “lock and key” model of receptor engagement, which serves as a predictive framework for the outcomes of drug interactions, whether therapeutic or adverse. This model is subject to ongoing optimization, thereby enhancing the precision and efficiency of drug development efforts.

Further enhancing this landscape is Computer-Aided Drug Design (CADD), which plays a pivotal role in refining Structure-based and Ligand-based Drug Design strategies. The SBDD is informed by detailed 3D structural analysis of biological targets, while LBDD compensates for the absence of structural data by focusing on the bioactivity of potential ligands. In computational chemistry, classical mechanics (MM and MD) and quantum mechanics (Ab Initio, semi-empirical, DFT) form the core methodologies. The MM and MD methods are advantageous in speed and capacity to handle complex molecules; however,

cannot calculate electronic interactions. In contrast, quantum mechanical methods provide a comprehensive understanding of molecular energetics and electronic structures but are resource-intensive, presenting a trade-off between speed and precision in drug design predictions.

Over the last ten years, this trade-off has been explored through a comprehensive review of FR research, highlighting considerable progress in developing folate-based drugs for cancer therapy, with an emphasis on the contributions of computational drug design. Key findings include the predominant use of molecular docking and dynamics simulations to understand drug-target interactions, with AutoDock Vina, Glide, and AutoDock GOLD emerging as accurate tools for docking. GROMACS stands out for molecular dynamics simulations, preferred for its efficiency and precision.

The research trajectory evolved from foundational analyses of FR interactions and binding modes to more complex strategies for selective drug uptake and detailed studies on molecular structures and interactions. Quantum mechanics advancements, like the SCC-DFTB approach, improved the accuracy of modeling biological systems. The use of Gaussian-type Orbitals (GTOs) with the 6–31G(d) basis set became common for calculating electronic structures, offering a balance between detail and computational manageability.

Recent years have seen a focus on enhancing drug specificity and selectivity, with computational methods evolving to provide deeper insights into molecular behavior. This decade of research has been pivotal in advancing cancer therapy through targeted drug delivery, leveraging computational techniques for more effective treatment solutions. However, while theoretical and computational advancements have been substantial, practical applications and experimental validations remain crucial for translating these findings into effective therapeutic strategies. Future research should focus on bridging the gap between computational predictions and real-world applications, emphasizing in vivo studies and clinical trials.

## Acknowledgements

A.J.J. and S.S.R. thank the Department of Science and Innovation and the Council for Scientific and Industrial Research for financial support.

## Conflict of Interest

The authors declare no conflict of interest.

## Author Contributions

A.J.J. and K.K.G. conceptualized the study and prepared the original draft. P.P.G. and S.S.R. provided expert opinions and critical reviews. All authors have read and agreed to the published version of the manuscript. A.J.J. and S.S.R. acquired funds.

## Keywords

classical mechanics, folate-based anticancer drugs, folate receptor, quantum mechanics

Received: April 18, 2024  
Revised: June 19, 2024  
Published online: July 7, 2024

- [1] O. Young, N. Ngo, L. Lin, L. Stanbery, J. F. Creeden, D. Hamouda, J. Nemunaitis, *Curr. Prob. Cancer* **2023**, *47*, 100917.
- [2] C. Martín-Sabroso, A. I. Torres-Suárez, M. Alonso-González, A. Fernández-Carballido, A. I. Fraguas-Sánchez, *Pharmaceutics* **2021**, *14*, 14.
- [3] Y. Shulpekova, V. Nechaev, S. Kardasheva, A. Sedova, A. Kurbatova, E. Bueverova, A. Kopylov, K. Malsagova, J. C. Dlamini, V. Ivashkin, *Molecules* **2021**, *26*, 3731.
- [4] S. B. Smith, P. S. Ganapathy, R. B. Bozard, V. Ganapathy, in *Handbook of Nutrition, Diet and the Eye*, Elsevier, Amsterdam **2014**, pp. 349–359.
- [5] M. Fernández, F. Javaid, V. Chudasama, *Chem. Sci.* **2018**, *9*, 790.
- [6] A. N. Tutt, A. Grigoriadis, A. Cheung, D. H. Josephs, G. Pellizzari, H. J. Bax, J. Bloomfield, J. F. Spicer, J. Opzomer, K. M. Ilieva, M. Figini, M. Fittall, S. Canevari, S. N. Karagiannis, *OncoTargets Ther.* **2016**, *7*, 52553.
- [7] P. Varaganti, V. Buddolla, B. A. Lakshmi, Y. J. Kim, *Life Sci.* **2023**, *326*, 121802.
- [8] M. J. Akhtar, M. Ahamed, H. A. Alhadlaq, S. A. Alrokayan, S. Kumar, *Clin. Chim. Acta* **2014**, *436*, 78.
- [9] P. Ebrahimnejad, A. Sodagar Taleghani, K. Asare-Addo, A. Nokhodchi, *Drug Discov. Today* **2022**, *27*, 471.
- [10] I. R. Vlahov, C. P. Leamon, *Bioconjug. Chem.* **2012**, *23*, 1357.
- [11] W. Wang, Z. Ye, H. Gao, D. Ouyang, *J. Control. Release* **2021**, *338*, 119.
- [12] Review of Data-Intensive Bioscience, *Biotechnology and Biological Sciences Research Council* **2020**.
- [13] X. Lin, X. Li, X. Lin, *Molecules* **2020**, *25*, 1375.
- [14] F. Jensen, *Introduction to Computational Chemistry*, John Wiley & Sons, Hoboken, NJ, USA, **2007**.
- [15] S. K. Singh, *Innovations and Implementations of Computer Aided Drug Discovery Strategies in Rational Drug Design*, Springer, Singapore **2021**.
- [16] A. Daina, M. C. Blatter, V. Baillie Gerritsen, P. M. Palagi, D. Marek, I. Xenarios, T. Schwede, O. Michielin, V. Zoete, *J. Chem. Educ.* **2017**, *94*, 335.
- [17] yourgenome, Image credit: Laura Olivares Boldú /Wellcome Connecting Science, <https://www.yourgenome.org/copyright-information/> (accessed: February 2024).
- [18] N. Singh, P. Vayer, S. Tanwar, J. L. Poyet, K. Tsaïoun, B. O. Villoutreix, *Front. Drug Discov.* **2023**, *3*, 1201419.
- [19] A. I. Visan, I. Negut, *Life* **2024**, *14*, 233.
- [20] H. P. Rang, *Br. J. Pharmacol.* **2006**, *147*, S9.
- [21] C. R. Prüll, A. H. Maehle, R. F. Halliwell, *A Short History of the Drug Receptor Concept*, Palgrave Macmillan UK, London **2009**, pp. 41.
- [22] E. J. Miller, S. L. Lappin, *Physiology, Cellular Receptor*, StatPearls, Treasure Island, FL, USA **2022**.
- [23] S. I. Berger, R. Iyengar, *WIREs Syst. Biol. Med.* **2011**, *3*, 129.
- [24] G. M. Currie, *J. Nucl. Med. Technol* **2018**, *46*, 81.
- [25] K. A. Berg, W. P. Clarke, *Int J Neuropsychopharmacol* **2018**, *21*, 962.
- [26] F. A. Holloway, J. M. Peirce, *Comprehensive Clinical Psychology*, Pergamon Press, Oxford **1998**, 173.
- [27] M. S. Salahudeen, P. S. Nishtala, *Saudi Pharm. J.* **2017**, *25*, 165.
- [28] P. M. Carron, A. Crowley, D. O'Shea, M. McCann, O. Howe, M. Hunt, M. Devereux, *Curr. Med. Chem.* **2018**, *25*, 2675.
- [29] C. Figliola, E. Marchal, B. R. Groves, A. Thompson, *RSC Adv.* **2019**, *9*, 14078.

- [30] OrgoSolver, <https://orgosolver.com/chapters/chapter-15/pka-and-electrical-properties-of-amino-acids> (accessed: March 2024).
- [31] M. Srinivasarao, C. V. Galliford, P. S. Low, *Nat. Rev. Drug Discov.* **2015**, *14*, 203.
- [32] A. Rana, S. Bhatnagar, *Bioorg. Chem.* **2021**, *112*, 104946.
- [33] P. V. Devarajan, P. Dandekar, A. A. D'souza, *Targeted Intracellular Drug Delivery by Receptor Mediated Endocytosis*, Springer Nature, Cham, Switzerland **2019**.
- [34] Y. G. Assaraf, C. P. Leamon, J. A. Reddy, *Drug Resist. Updat* **2014**, *17*, 89.
- [35] M. Jurczyk, K. Jelonek, M. Musiał-Kulik, A. Beberok, D. Wrześniok, J. Kasperczyk, *Pharmaceutics* **2021**, *13*, 326.
- [36] A. Tucak-Smajić, Scientific Image and Illustration Software | BioRender, <https://www.biorender.com/> (accessed: April 2024).
- [37] V. Sharma, S. Wakode, H. Kumar, *Cheminformatics and Bioinformatics in the Pharmaceutical Sciences*, Elsevier, Amsterdam **2021**, pp. 27–53.
- [38] G. L. Wilson, M. A. Lill, *Future Med. Chem.* **2011**, *3*, 735.
- [39] N. Astalakshmi, T. Gokul, K. B. Gowri Sankar, M. Nandhini, M. R. Hari Hara Sudhan, S. Gowtham, S. T. Latha, M. S. Kumar, *Int. J. Pharm. Sci. Rev. Res.* **2022**, *77*, 108.
- [40] A. Tripathi, K. Misra, *JSM Bioinform. Genom. Proteom.* **2017**, *2*, 1015.
- [41] M. Batool, B. Ahmad, S. Choi, *Int. J. Mol. Sci.* **2019**, *20*, 2783.
- [42] I. J. dos S Nascimento, T. M. de Aquino, E. F. da Silva-Júnior, *Lett. Drug Des. Discov.* **2022**, *19*, 951.
- [43] M. K. Mahapatra, M. Karuppasamy, *Computer Aided Drug Design (CADD): From Ligand-Based Methods to Structure-Based Approaches*, Elsevier, Amsterdam, **2022**, pp. 17–55.
- [44] C. Acharya, A. Coop, J. E. Polli, A. D. MacKerell, *Curr. Comput. Aided Drug Des.* **2011**, *7*, 10.
- [45] C. Mealli, **2006**, <https://doi.org/10.13140/2.1.1878>.
- [46] A. Rimola, S. Ferrero, A. Germain, M. Corno, P. Ugliengo, *Minerals* **2020**, *11*, 26.
- [47] T. Vreven, K. Morokuma, Ö. Farkas, H. B. Schlegel, M. J. Frisch, *J. Comput. Chem.* **2003**, *24*, 760.
- [48] G. J. Cheng, X. Zhang, L. W. Chung, L. Xu, Y. D. Wu, *J. Am. Chem. Soc.* **2015**, *137*, 1706.
- [49] Y. Wang, J. Fass, B. Kaminow, J. E. Herr, D. Rufa, I. Zhang, I. Pulido, M. Henry, H. E. Bruce Macdonald, K. Takaba, J. D. Chodera, *Chem. Sci.* **2022**, *13*, 12016.
- [50] O. A. Arodola, M. E. S. Soliman, *Drug Des. Devel. Ther.* **2017**, *11*, 2551.
- [51] J. A. McCammon, B. R. Gelin, M. Karplus, *Nature* **1977**, *267*, 585.
- [52] A. Hospital, J. R. Goñi, M. Orozco, J. L. Gelpí, *Adv. Appl. Bioinform. Chem.* **2015**, *8*, 37.
- [53] A. Pérez, F. Lankas, F. J. Luque, M. Orozco, *Nucleic Acids Res.* **2008**, *36*, 2379.
- [54] M. S. Badar, S. Shamsi, J. Ahmed, M. A. Alam, *Integrated Science* **2022**, 131.
- [55] O. M. H. Salo-Ahen, I. Alanko, R. Bhadane, A. M. Alexandre, R. V. Honorato, S. Hossain, A. H. Juffer, A. Kbedev, M. Lahtela-Kakkonen, A. S. Larsen, E. Lescrier, P. Marimuthu, M. U. Mirza, G. Mustafa, A. Nunes-Alves, T. Pantsar, A. Saadabadi, K. Singaravelu, M. Vanmeert, *Processes* **2021**, *9*, 71.
- [56] W. F. van Gunsteren, H. J. C. Berendsen, *Angew. Chem. Int. Ed. Engl.* **1990**, *29*, 992.
- [57] B. Roux, T. Simonson, *Biophys. Chem.* **1999**, *78*, 1.
- [58] M. Orozco, F. J. Luque, *Chem. Rev.* **2000**, *100*, 4187.
- [59] T. Luchko, S. Gusarov, D. R. Roe, C. Simmerling, D. A. Case, J. Tuszynski, A. Kovalenko, *J. Chem. Theory Comput.* **2010**, *6*, 607.
- [60] R. Pino-Rios, O. Yañez, D. Inostroza, R. Báez-Grez, C. Cárdenas, W. Tiznado, *Chemical Reactivity*, Vol. 2, Elsevier, Amsterdam **2023**.
- [61] K. Ohno, H. Satoh, *Theo. Comp. Chem. Series, Chapter 2*, RCS, Cambridge **2022**, pp. 17–68.
- [62] A. Tran, L. He, Y. Wang, *ASME J. Risk Uncertainty Part B. Mech. Eng.* **2018**, *4*, 011006.
- [63] S. Waclawek, *Ecol. Chem. Eng. S* **2021**, *28*, 11.
- [64] S. McArdle, S. Endo, A. Aspuru-Guzik, S. C. Benjamin, X. Yuan, *Rev. Mod. Phys.* **2020**, *92*, 015003.
- [65] F. Agostini, B. F. E. Curchod, *Philos Trans A Math Phys Eng Sci* **2022**, *380*, 0375.
- [66] M. Stanke, *Handbook of Computational Chemistry*, Springer International Publishing, Cham, Switzerland **2017**, pp. 173–223.
- [67] B. Nagy, F. Jensen, *Reviews in Computational Chemistry*, Wiley, New York **2017**, 30.
- [68] F. Jensen, *WIREs Comput. Mol. Sci.* **2013**, *3*, 273.
- [69] J. Pokluda, M. Černý, M. Šob, Y. Umeno, *Prog. Mater. Sci.* **2015**, *73*, 127.
- [70] E. G. Lewars, *Computational Chemistry Introduction to the Theory and Applications of Molecular and Quantum Mechanics*, Springer, Berlin, Germany, **2016**.
- [71] A. M. Sapse, in *Molecular Orbital Calculations for Biological Systems*, Oxford University Press, Oxford, UK **1998**.
- [72] R. Izsák, A. V. Ivanov, N. S. Blunt, N. Holzmann, F. Neese, *J. Chem. Theory Comput.* **2023**, *19*, 2703.
- [73] BULTINCK, *Computational Medicinal Chemistry for Drug Discovery*, Marcel Dekker, New York, NY **2003**.
- [74] A. S. Christensen, T. Kubař, Q. Cui, M. Elstner, *Chem. Rev.* **2016**, *116*, 5301.
- [75] M. Orio, D. A. Pantazis, F. Neese, *Photosynth. Res.* **2009**, *102*, 443.
- [76] M. Aamir Iqbal, N. Ashraf, W. Shahid, D. Afzal, F. Idrees, R. Ahmad, *Density Functional Theory – Recent Advances, New Perspectives and Applications*, IntechOpen, London, UK, **2022**.
- [77] E. K. U. Gross, W. Kohn, *Phys. Rev. Lett.* **1985**, *55*, 2850.
- [78] J. P. Perdew, W. Yue, *Phys. Rev. B* **1986**, *33*, 8800.
- [79] J. P. Perdew, Y. Wang, *Phys. Rev. B* **1992**, *45*, 13244.
- [80] P. Pulay, S. Saebø, *Theor. Chim. Acta* **1986**, *69*, 357.
- [81] L. Goerigk, S. Grimme, *WIREs Comput. Mol. Sci.* **2014**, *4*, 576.
- [82] S. F. Sousa, P. A. Fernandes, M. J. Ramos, *J. Phys. Chem. A* **2007**, *111*, 10439.
- [83] P. Verma, D. G. Truhlar, *Trends Chem.* **2020**, *2*, 302.
- [84] N. Mardirossian, M. Head-Gordon, *Mol. Phys.* **2017**, *115*, 2315.
- [85] E. G. Lewars, *Computational Chemistry Introduction to the Theory and Applications of Molecular and Quantum Mechanics*, Springer, Dordrecht, Netherlands **2010**.
- [86] H. Dorsett, A. White, Overview of Molecular Modelling and Ab Initio Molecular Orbital Methods Suitable for Use with Energetic Materials **2000**.
- [87] T. GUND, *Guidebook on Molecular Modeling in Drug Design*, Elsevier, Amsterdam **1996**, pp. 55–92.
- [88] P. C. Agu, C. A. Afukwa, O. U. Orji, E. M. Ezeh, I. H. Ofoke, C. O. Ogbu, E. I. Ugwuja, P. M. Aja, *Sci. Rep.* **2023**, *13*, 13398.
- [89] X. Y. Meng, H. X. Zhang, M. Mezei, M. Cui, *Curr. Comput. Aided Drug Des.* **2012**, *7*, 146.
- [90] D. B. Kitchen, H. Decornez, J. R. Furr, J. Bajorath, *Nat. Rev. Drug Discov.* **2004**, *3*, 935.
- [91] R. N. Sahoo, S. Pattanaik, G. Pattnaik, S. Mallick, R. Mohapatra, *Indian J Pharm Sci* **2022**, *84*, 1334.
- [92] A. K. Padhi, M. Janežič, K. Y. J. Zhang, *Advances in Protein Molecular and Structural Biology Methods*, Elsevier, Amsterdam **2022**, pp. 439–454.
- [93] J. Lee, X. Cheng, J. M. Swails, M. S. Yeom, P. K. Eastman, J. A. Lemkul, S. Wei, J. Buckner, J. C. Jeong, Y. Qi, S. Jo, V. S. Pande, D. A. Case, C. L. Brooks, A. D. MacKerell, J. B. Klauda, W. Im, *J. Chem. Theory Comput.* **2016**, *12*, 405.
- [94] 20 Best Software for Molecular Modeling and Simulations in Academia 2024, <https://www.scijournal.org/articles/best-software-for-molecular-modeling-and-simulations>, (accessed: February 2024).

- [95] C. Wang, Y. Jiang, X. Fei, Y. Gu, *J. Phys. Org. Chem.* **2018**, *31*, e3719.
- [96] C. Wang, Y. Jiang, M. Zhang, X. Fei, Y. Gu, *J. Mol. Graph. Model.* **2018**, *85*, 40.
- [97] Y. Jiang, C. Wang, M. Zhang, X. Fei, Y. Gu, *J. Mol. Graph. Model.* **2020**, *100*, 107663.
- [98] M. Elstner, *Theor. Chem. Acc.* **2006**, *116*, 316.
- [99] R. L. Harrison, *AIP Conf. Proc.* **2010**, *1204*, 17.
- [100] J. Siepmann, F. Siepmann, *Int. J. Pharm.* **2008**, *364*, 328.
- [101] A. Erdemir, T. M. Guess, J. Halloran, S. C. Tadepalli, T. M. Morrison, *J. Biomech.* **2012**, *45*, 625.
- [102] J. Zhou, S. Vijayavenkataraman, *Pharmaceutics* **2022**, *14*, 230.
- [103] R. E. Amaro, A. J. Mulholland, *Nat. Rev. Chem.* **2018**, *2*, 0148.
- [104] A. N. Lima, E. A. Philot, G. H. G. Trossini, L. P. B. Scott, V. G. Maltarollo, K. M. Honorio, *Expert Opin. Drug Discov.* **2016**, *11*, 225.
- [105] A. Shahiwala, *A Handbook of Artificial Intelligence in Drug Delivery*, Elsevier, Amsterdam **2023**, pp. 83–96.
- [106] L. K. Golani, C. George, S. Zhao, S. Raghavan, S. Orr, A. Wallace, M. R. Wilson, Z. Hou, L. H. Matherly, A. Gangjee, *J. Med. Chem.* **2014**, *57*, 8152.
- [107] S. Della-Longa, A. Arcovito, *J. Comput. Aided Mol. Des.* **2015**, *29*, 23.
- [108] D. Sampogna-Mireles, I. D. Araya-Durán, V. Márquez-Miranda, J. A. Valencia-Gallegos, F. D. González-Nilo, *J. Mol. Graph. Model.* **2017**, *72*, 201.
- [109] E. Nogueira, M. P. Sárria, N. G. Azoia, E. Antunes, A. Loureiro, D. Guimarães, J. Noro, A. Rollett, G. Guebitz, A. Cavaco-Paulo, *Biochemistry* **2018**, *57*, 6780.
- [110] S. Iliev, G. Gocheva, N. Ivanova, B. Atanasova, J. Petrova, G. Madjarova, A. Ivanova, *Phys. Chem. Chem. Phys.* **2018**, *20*, 28818.
- [111] L. Xing, Y. Xu, K. Sun, H. Wang, F. Zhang, Z. Zhou, J. Zhang, F. Zhang, B. Caliskan, Z. Qiu, M. Wang, *Sci. Rep.* **2018**, *8*, 3426.
- [112] F. Abyar, I. Novak, *J. Mol. Liq.* **2019**, *276*, 819.
- [113] J. Petrova, G. Gocheva, N. Ivanova, S. Iliev, B. Atanasova, G. Madjarova, A. Ivanova, *J. Mol. Graph. Model.* **2019**, *87*, 172.
- [114] Y. Jiang, C. Wang, M. Zhang, X. Fei, Y. Gu, *J. Mol. Graph. Model.* **2019**, *87*, 121.
- [115] G. Gocheva, N. Petkov, A. Garcia Luri, S. Iliev, N. Ivanova, J. Petrova, Y. Mitrev, G. Madjarova, A. Ivanova, *J. Mol. Liq.* **2019**, *292*, 111392.
- [116] G. Gocheva, N. Ivanova, S. Iliev, J. Petrova, G. Madjarova, A. Ivanova, *J. Chem. Theory Comput.* **2020**, *16*, 749.
- [117] S. Kunjiappan, S. Govindaraj, P. Parasuraman, M. Sankaranarayanan, S. Arunachalam, P. Palanisamy, U. P. Mohan, E. Babkiewicz, P. Maszczyk, S. Vellaisamy, T. Panneerselvam, *Nanotechnology* **2020**, *31*, 155102.
- [118] A. Thamarai, R. Vadamar, M. Raja, S. Muthu, B. Narayana, P. Ramesh, R. R. Muhamed, S. Sevvanthi, S. Aayisha, *Spectrochim. Acta A Mol. Biomol. Spectrosc.* **2020**, *226*, 117609.
- [119] M. G. Al-Thiabat, A. M. Gazzali, N. Mohtar, V. Murugaiyah, E. E. Kamarulzaman, B. K. Yap, N. A. Rahman, R. Othman, H. A. Wahab, *Molecules* **2021**, *26*, 5304.
- [120] M. G. Al-Thiabat, F. G. Saqallah, A. M. Gazzali, N. Mohtar, B. K. Yap, Y. S. Choong, H. A. Wahab, *Molecules* **2021**, *26*, 1079.
- [121] E. N. Schaber, N. Ivanova, S. Iliev, J. Petrova, G. Gocheva, G. Madjarova, A. Ivanova, *J. Phys. Chem. B* **2021**, *125*, 7598.
- [122] C. Wang, M. Zhang, S. Shi, Y. Jiang, X. Fei, L. Liu, D. Ye, S. Zhang, *J. Mol. Model.* **2022**, *28*, 205.
- [123] S. Sarwar, M. A. Qadir, R. D. Alharthy, M. Ahmed, S. Ahmad, M. Vanmeert, M. U. Mirza, A. Hameed, *Molecules* **2022**, *27*, 1780.
- [124] P. Mazumdar, A. Kashyap, D. Choudhury, G. Borgohain, *Chemistry-Select* **2022**, *7*, 202203588.
- [125] M. Yusuf, G. Dwi Pramono, Z. Nafisah, A. Rizqi Ridwan Firdaus, A. Hardianto, V. Yulianti Susilo, A. Mutalib, U. M. Soedjanaatmadja, *Indones. J. Comput. Biol. (IJCB)* **2022**, *1*, 22.



**Andrea Josiah** is a research scientist at the Council for Scientific and Industrial Research (CSIR), South Africa. She obtained a Master's degree in Chemical Sciences from the University of Johannesburg in 2021. She is currently completing her PhD which focuses on developing targeted drug delivery systems for cancer treatment. Her research employs computational chemistry to aid the design of nanoparticles and small-molecule drug conjugates for applications in healthcare. She has been inducted into the Golden Key International Honor Society, awarded first prize at the South African Society for Microbiology, and received various scholarships.



**Krishna K. Govender** is a Senior Lecturer in the Department of Chemical Sciences at the University of Johannesburg. Apart from lecturing organic, inorganic, and physical chemistry at the undergraduate and honors levels, his research focuses on Computational Chemistry and Material Science, in the field of drug design. His research group focuses on: Quantum Mechanics (QM), Molecular Mechanics (MM), Molecular Dynamics (MD), and hybrid QM/MM. He has ongoing collaborations with the University of KwaZulu-Natal, Durban University of Technology, University of Fort Hare, University of Cape Town, Cape Peninsular University of Technology, Stellenbosch University, and University of Sri Jayewardenepura.



**Penny Govender** has been with the University of Johannesburg since 2002, transitioning from an academic in the Faculty of Science to the Director of the Research Capacity Development unit in January 2022, and currently serving as the Senior Director of the Postgraduate School. Her research in computational chemistry includes energy, water, materials science, and disease, resulting in over 100 publications and 11 book chapters. Govender has supervised numerous postdoctoral fellows and graduate students. Her notable recognitions include induction as a Fellow of the Royal Society of Chemistry in 2023, and she actively participates in securing research funding.



**Suprakash Sinha Ray** is the Chief Research Scientist and Director of the DST/CSIR National Centre for Nanostructured Materials in Pretoria, South Africa. His research centers on advanced nanostructured and polymeric materials. Recognized as one of the top 1% most impactful scientists by Thomson Reuters, he is a leading author in polymer nanocomposite materials. Prof. Ray has authored five books, co-edited three books, and published over 330 journal articles and 32 book chapters. He holds professorships at the University of Pretoria and the University of Johannesburg and serves on the editorial boards of several prestigious journals.